The BMP4-BMPR1A axis represses BRCA1, inducing BRCAness in mammary stem cells and contributing to tumor initiation in basal-like breast cancer

Simon AHO[,2,3,4,5], Marie PERBET[,2,3,4], Isabelle TREILLEUX[6], Adrien BUISSON[6], Sandrine JEANPIERRE[,2,3,4], Emmanuel DELAY[1,2,3,4,8], Véronique MAGUER-SATTA[1,2,3,4,&*] and Boris GUYOT[1,2,3,4,&*]

[1]CNRS UMR5286, Centre de Recherche en Cancérologie de Lyon, F-69000 Lyon, France; [2]Inserm U1052, Centre de Recherche en Cancérologie de Lyon, F-69000 Lyon, France; [3]Université de Lyon, F-69000, Lyon, France; [4]Université de Lyon 1, ISPB, F-69000, Lyon, France; [5]Centre Léon Bérard, Département de Cancérologie Médicale, Lyon, F-69008, France; [6]Centre Léon Bérard, Département de Biopathologie. Lyon, F-69008, France; [7] Centre Léon Bérard, Département de Biopathologie. Lyon, F-69008, [8]Centre Léon Bérard, Département de Chirurgie, Lyon, F-69008, France ;

Correspondence Footnote : [&]These authors contributed equally ; *****Correspondence and requests should be addressed to Véronique MAGUER-SATTA or Boris GUYOT, Cancer Research Center of Lyon-CRCL, U1052-UMR5286, 28 rue Laennec, 69373 Lyon Cedex 08, FRANCE, 33-478 782 907, Fax 33- 478 782 720, veronique.maguer-satta@lyon.unicancer.fr ; boris.guyot@lyon.unicancer.fr

Running Title: BMP, BRCA and breast cancer stem cells**;**

Abstract

Basal-like breast cancer (BLBC) is an aggressive subtype frequently characterized by homologous recombination deficiency (HRD) and BRCAness, even in the absence of BRCA1 mutations. Here, we identify the BMP4-BMPR1A signaling axis as a novel regulator of BRCA1 expression and a driver of BRCAness in non-transformed immature mammary cells. Analyses of patient samples reveal that high BMPR1A expression correlates with low BRCA1 levels and poor prognosis in BLBC. We show that BMP4 exposure induces BRCA1 transcriptional repression via BMPR1A, promoting a basal differentiation and impairing homologous recombination. This results in increased sensitivity to PARP inhibitors (PARPi) and accumulation of genetically unstable, immature cells. In addition, long-term BMP4 stimulation or BMPR1A overexpression induces transformation. Our findings uncover a mechanism by which the tumor microenvironment could contributes to BLBC initiation through BMP4-induced suppression of BRCA1, and suggest BMP signaling and the resultant BRCAness as a therapeutic vulnerability in BRCA1 wild-type BLBCs.

Introduction

Breast cancer is a heterogeneous disease with several molecular subtypes, each subtype being associated with a specific gene expression profile in the so-called intrinsic classification. According to this transcriptomic classification, luminal A, luminal B, normal-like, HER2 enriched and basal-like subtypes can be distinguished[1–3]. Basal-like breast cancer (BLBC) accounts for approximately 20% of breast cancer cases[3–5] and is associated with the poorest prognosis, particularly in terms of age at diagnosis and survival[6–9]. BLBC strongly expresses a number of genes also expressed by myoepithelial cells as well as progenitors and mammary stem cells located in the outer (basal) layer of the mammary gland [10]. Other genes involved in epithelial-mesenchymal transition (EMT), proliferation or stemness are also overexpressed[1,3]. Conversely, genes encoding estrogens receptor (ERα), progesterone receptor (PR) and Human Epidermal Growth Factor Receptor-2 (HER2) are weakly expressed in

BLBCs[1,3], resulting in a frequent triple-negative (TNBC) phenotype (absence of ERα and PR expression, absence of HER2 amplification/overexpression)[6,11]. Beyond these transcriptomic characteristics, BLBCs display other histo-molecular features contributing to their aggressiveness. At the molecular level, most BLBCs show specific mutational patterns and chromosomal rearrangements related to alterations in homologous recombination (HR)[12], a DNA double-strand break repair pathway essential for maintaining genome stability. It is an error-free process that uses the sister chromatid of the damaged chromatid as a template to restore its integrity[13]. HR involves a large number of proteins that interact with each other and with the damaged DNA. Among genes encoding these proteins, BRCA1 and BRCA2 are the best known because their germline mutations are associated with an increased risk of ovarian and breast cancers[14]. However, other homologous recombination deficiency (HRD) mechanisms have been described beyond the BRCA1/2 germline mutations, leading to a "BRCAness" situation, i.e. a phenocopy of these inherited mutations[15]. Depending on the studies and HRD detection techniques considered, up to 80% of BLBCs are thought to be HRD[12,16–18]. Some causes of HRD are well documented in these tumors including germline (10% of cases) or somatic (6%) BRCA1 mutations, germline (2.5%) or somatic (2.5%) BRCA2 mutations[19], BRCA1 promoter hypermethylation (14[20]-34%[21]) or ID4 over expression (37.5-50%)[22]. Mechanisms of transcriptional or post-transcriptional repression involving for example certain miRNAs directed against BRCA1 transcript have also been described[23–27]. However, if many processes seem to be at the origin of BRCAness in BLBCs their molecular mechanisms remain largely unexplored. Interestingly, several studies have shown *in vitro* that some cytokines of the tumor microenvironment (TME), such as the TGFβ could repress some HR genes in tumors[28,29] suggesting that in basal-like carcinogenesis, some TME stresses could contribute to the acquisition of an HRD phenotype. Histologically, BLBCs are characterized by high expression of basal cytokeratins (CK5/6, CK14, CK17) and of EGFR[30,31]. They are high-grade proliferative tumors with high mitotic index and high intra-tumor heterogeneity[31]. Interestingly, enrichment of cancer stem cells (CSC) with a CD44+/CD24- phenotype is also observed[32]. These cells share self-renewal and differentiation properties with normal mammary stem cells (MaSC), but also display tumorigenic and treatment-resistant properties.

Therefore CSC are involved not only at early stages of tumorigenesis but also during progression and at relapse in a number of cancers, such as breast carcinomas[33]. It has been proposed that mammary stem cells or an ER^- luminal progenitor could be the target of transormation[34,35]. Despite these elements, the question of the cell of origin in BLBC is still controversial and remained to be elucidated. In this context, the Bone Morphogenetic Pathway (BMP) signaling control MaSC homeostasis cell fate toward both mammary epithelial cell types[36,37]. The BMP belong to the TGFβ superfamily and are produced by the mammary gland microenvironment. Organized in homo or heterocomplexes, they exert their functions by binding to their receptors classically organized in tetramers (2 type I receptors and 2 type II receptors with serine-threonine kinase activity able to initiate signal transduction)[38]. The signal is then further transduced through a canonical pathway involving SMAD1/5/8 phosphorylation and their binding to SMAD4 forming a transcriptionally active complex in the nucleus. There is also a SMAD independent non-canonical pathway involving the activation of certain MAP kinases such as ERK, JNK or p38[39]. BMP pathway dysregulations have been described in luminal breast cancers tumorigenesis[36]. However, the involvement of this signaling pathway specifically in BLBC carcinogenesis has been poorly explored, even if the role of BMPR1A and BMP4 has been suggested by a few studies[40,41]. Here we show that the BMP4/BMPR1A signaling decreases BRCA1 gene expression, resulting in an increased basal differentiation of mammary progenitors and in an HR impairment associated with genomic instability and transformation.

Materials and methods

Cell culture

The MCF10A human untransformed immature mammary epithelial cell model was used because these cells are functionally representative of the behavior of healthy MaSCs as previously described. This cell line was purchased from the American Type Culture Collection (ATCC, USA) and cultured according to recommendations in Dulbecco's Modified Eagle's Medium (DMEM)/F-12 nutrient mix supplemented with 1% Penicillin/Streptomycin (Life Technologies), 1%GlutaMAx (Thermo Fisher), 5% Horse Serum

(Life Technologies), 10 ug/ml Insulin (Novorapid), 0.5 ug/ml Hydrocortisone (Sigma), 100ng/ml Cholera Toxin (Sigma) and 20 ng/ml Epithelial Growth Factor (EGF) (Sigma). Cells were incubated with 5% CO2 at 37°C. The cell lines were tested negative for mycoplasma contamination before conducting the experiments.

Generation of cell lines

The MCF10A cell line with BRCA1 knockdown was generated using an all-in-one Tet-ON lentiviral transfected system. The transfected vector construct contained a shRNA sequence complementary to the target messengerRNA (BRCA1 or luciferase for the control cell line). Upstream was located a GFP coding sequence (allowing the transfection efficiency control), followed by a Puromycin (Puro) resistant gene constitutively expressed thanks to the PGK promoter. This enabled the selection of the successfully transfected cells with 0,5 ug/ml Puro treatment for 4 days in the MCF10A cells medium. Pooled resistant clones were then treated with an overnight pulse of 400 ng/ml Doxycycline (Dox) to induce the expression of shRNAs along with GFP protein. The GFP positive cells, i.e. able to respond to Dox, were sorted using Fluorescence-activated cell sorting (FACS) (see below) and expanded so as to form the different required conditions: shBRCA1 and shLuciferase (shLuc) i.e. shControl.

Overexpressing BMPR1A MCF10A and its related control were obtained after transfection and Puro selection (0,5 ug/ml) of MCF10A cells with a BMPR1A WT (pcDNA3-HA-BMPRIA WT) obtained from Ten Dijke/Heldin team (for overexpressing BMPR1A MCF10A) or with a control empty construct.

To generate MCF10A-FUCCI cell lines, fucci constructs (mVenus-hGeminin/pcDNA3 and mCherry-hCdt1/pcDNA3) obtained from Riken Institute were transfected into MCF10A cell line and selected with Puro (1ug/ml).

In silico analysis

Different cohorts were used for in silico analyses: TCGA-Breast cancer, GTEx, GOBO. Transcriptional expression analysis of BMPR1A, BMPR1B, BMP2, BMP4 in the different molecular subtypes of breast cancer and non-tumoral controls was performed using the Breast Cancer Gene-Expression Miner v5.0

(bc-GenExMiner v5.0) and the Gene Expression-Based Outcome for Breast Cancer Online (http://co.bmc.lu.se/gobo) tools. Correlation analyses were performed using bc-GenExMiner v5.0. Overall survival analyses were performed using km plotter (https://kmplot.com/analysis/)

Quantification of soluble BMP4 in primary tissues

To determine the concentration of secreted BMP4 in the microenvironment of primary tissue samples, standardized normal and tumor tissue supernatants were prepared as described previously[36]. Supernatants were filtered using a 40 mM cell strainer and used to quantify soluble BMP4. ELISA quantifications of BMP4 were performed following the manufacturer's instructions (Quantikine ELISA Kit; R&D Systems).

Reverse transcription and Quantitative Polymerase Chain Reaction

Total RNA was extracted using Rneasy Mini Kit (Qiagene®) following the protocol from the manufacturer. The quantity of RNA was determined using a Nanodrop spectrophotometer (Thermo Fisher Scientific). 1 ug of extracted RNA samples were used for the synthesis of cDNA using the SuperScript™ RT reagent kit (Takara). The samples were incubated at 25°C for 10 minutes, followed by another incubation at 42°C for 50 minutes and inactivated at 70°C for 15 minutes. The cDNA was diluted four times with Rnase-free water. 2 ul of cDNA was subjected to q-PCR using the QuantiFast SYBR® Green RT-PCR Kit (Qiagene®). The reaction consisted of an incubation at 95°C for 5 minutes, followed by 45 cycles of 95°C and 60°C incubations for 10 and 30 seconds respectively. Negative controls (no template or no reverse transcriptase) were included. The CT values were used to calculate the fold difference in the target gene with relative to the endogenous house-keeping gene CPB.

Western-blot

Protein samples were collected in Laemmli buffer (0.05M Tris (pH 6.8), 2% SDS, 2,5% β-mercaptoethanol and 5% glycerol). In each experimental condition, the same number of cells was collected to obtain a similar protein concentration in each sample. Samples were boiled for 5 min at

100°C and sonicated for around 10 secondes. The 10% SDS– PAGE gradient gels were run in running buffer (25 mM Tris, 192 mM glycine, 0,1% SDS) and transferred to PVDF membranes in transfer buffer (Transfer buffer (Biorad), 20% ethanol). Membranes were blocked in 5% BSA in TBS-T buffer (Tris-buffered saline 10X (Euromedex) containing 1% Tween-20 (Euromedex). Primary antibodies were incubated overnight at 4 °C and washed with TBS-T buffer. HRP-conjugated secondary antibodies were left at room temperature for 1 h and washed with TBS-T buffer. Western blot development was performed using Clarity™ Western ECL Substrate (Biorad) and Chemidoc™ Imaging System (Biorad).

-Primary antibodies and dilution factors :

Mouse-Anti BRCA1 (Merck Op92-100, 1/500)

Rabbit-Anti cleaved caspase 3 (Cell signaling 9661 (1/1000)

Mouse-Anti GAPDH (Abcam Ab8245, 1/10000)

Rabbit-Anti βtubulin (Abcam, Ab6046, 1/2000)

Fluorescence-activated cell sorting

The different MCF10A shRNA cell lines to be sorted were cultured in 6-well plates in the MCF10A cells medium with the addition of Puro 0.5 ug/ml for 4 days to select efficiently transfected cells and 400ng/ml Dox the day before sorting to induce shRNA and GFP expression. The cells were collected at 85% confluence, rinsed with PBS 1X (Gibco), trypsinized, centrifuged at 1200g for 5 minutes and the cell pellets were resuspended in PBS 1X containing 1% fetal calf serum. Sorting was performed using a BioRad S3e cell sorter.

Flow cytometry

Cytometric analysis of cells was performed on an LSRFortessa cytometer. The software Diva was used for acquisition and Flow-Jo for analysis.

Epithelial Colony Forming Cell (E-CFC) assay

On the day of the assay, 30Gy previously irradiated NIH3T3 feeder cells were thawed and seeded in 12-well plates at a density of 8.10^4 cells/well in the MCF10A cells medium in order to provide differentiation factors for MCF10A cells. Following this, 250 to 500 cells of interest were added at limiting dilution into each well. After 7 days of co-culture, different colonies emerge depending on the differentiation program activated by the cells: luminal, basal and mixed. The colonies formed were fixed with ice-cold methanol, visualized using Wright's stain (Sigma-Aldrich) and counted under an Olympus microscope at 4X magnification. The colonies were then classified (luminal/basal/mixed) according to their previously described morphological features[98].

Mammosphere assay

Cells of interest were cultured in 96-well ultra-low attachment plates in serum free mammary epithelial cell basal growth medium (MEBM) supplemented with B27 (a serum-free supplement from thermo-Fisher), 4 mg/ml heparin (Life Technologies), 20 ng/ml basic EGF (Life Technologies). There were 8 wells for each condition. After 6 days, the spheres formed were counted under a 4X ZEISS microscope.

Soft Agar Assay

This assay is based on the colony-like growth of transformed cells cultured in a specific soft agar medium. The bottom agar layer was prepared from 3% agar diluted in culture medium to reach a final concentration of 1,5%. 1 mL was added to 12-well cell culture plates and incubated at room temperature for 1 hour. The top agar layer was added on top of the bottom agar at a final concentration of 15000 cells/well in 1 mL. Each condition was performed in triplicate. Cell culture plates were incubated at room temperature for 30 min before incubation at 5% CO2 and 37°C. Colonies were quantified after 3 weeks.

Immunohistochemistry

IHC analyses were performed on previously untreated triple-negative breast cancer cases selected from a pre-established tissu-microarray. H&E and IHC staining of paraffin sections of breast tumors was carried out using standard methods and the following antibodies: BMPR1A (MA5-17036, Invitrogen), BMP2 (ab124715, Abcam), and CK14 (06 732 429 001, Roche diagnostics). The number of positive cells for each marker and the staining intensity on a quantitative scale from 0 to 3 were determined. An expression score was defined as the product of these two parameters.

Comet assay

The first steps are common to both neutral and alkaline comet assays. Cells of interest from the different experimental conditions were diluted in ion-free 1X PBS to a concentration of 1.5x10^6/ml. 12.5 ul of this cell suspension was diluted in 125 ul of Trévigen 1% Agarose LMPA. 40 ul of the mix was spread on a microscope slide placed on a hot plate at 37° before incubation for 30 min at 4° in a dark, humid chamber. The slides were then immersed in a lysis solution (Trevigen) at 4° for 1 hour. For the neutral comet assay, slides were incubated in 1X neutral electrophoresis buffer at 4° for 30 min, then placed in the electrophoresis tank with 850 ml of 1X neutral electrophoresis buffer for 45 min migration at 21 volts and 4°. The slides were then placed in a precipitation solution for 30 min at room temperature, incubated for 30 min in 70% ethanol and dried. Finally, the slides were incubated in a Sybr Gold solution for 30 minutes at room temperature, then mounted with fluoromount medium. Slides were then read under a ZEISS epifluorescence microscope using the Cy3 laser and analyzed on imageJ using the opencomet program. For the alkaline comet assay, slides were incubated in alkaline buffer at 4° for 40 min overnight, then placed in the electrophoresis tank with 850 ml of 1X alkaline buffer for 30 min migration at 25 volts and 4°. The slides were then placed in a neutralization solution for 10 min at 4° (repeated 3 times), incubated for 30 min in 70% ethanol and dried. Finally, the slides were incubated in a Sybr Gold solution for 30 minutes at room temperature, then mounted with fluoromount medium. Slides were then read under a ZEISS epifluorescence microscope using the Cy3

laser and analyzed on imageJ using the opencomet program. The composition and concentration of the various solutions and buffers are indicated on the trvigen kit.

Statistical analysis

Regarding the relationships between BRCA1 transcriptional and BMPR1A and BMP4 protein expression: The relationships between BRCA1 transcriptional expression and its potential predictors (membrane BMPR1A, overall BMPR1A, and cytosolic BMP4 protein expression) were modeled using linear regression. A potential non-linear relationship was first investigated using fractional polynomials. Possible confounding factors such as age at diagnosis, stage, and CK14 positivity were accounted for through bivariate regression analysis due to the small sample size. A robust variance estimator was used. A sensitivity analysis was conducted using median regression. Finally, given the sample size, a Bayesian analysis was also performed. It comprised three components:

1. A confirmatory linear regression model.
2. A Bayesian Model Averaging approach to identify the most plausible models given the data.
3. An estimation of Bayes factors to quantify the evidence provided by the data in favor of one statistical model over another.

Stata software (version 18) (Stata 2023) and R (R Core Team 2023) were used for the analyses.

Regarding differentiation: The relationship between experimental conditions and differentiation was estimated using a generalized negative binomial regression model. A robust variance estimator was used to account for correlated data (repeated measures). The presence of potential interactions between experimental conditions and differentiation was tested. Multiple comparisons were performed via marginal effect analysis, taking into account Bonferroni and Sidak tests. The goodness of fit of the data to the model was verified. Stata software (version 15) was used. Regarding the dose-response relationship: Different models with three, four, or five parameters (ED50 being one of them) were estimated using a nonlinear regression model. These included logistic, log-logistic, Weibull, and other models. A mixed model (also called a hierarchical model) was used to account for repeated

measurements, as a sensitivity analysis. The principle of parsimony was used to select the most adequate model. The drc package of R software was used.

Other statistical analyses were essentially carried out using student's T-test or ANOVA according to experimental situation. The statistical analyses and graphs were performed with Graphpad Prism (version 8). Significant P values are given in the text or symbolized by asterisks (*p<0,05 ; **p<0,01 ; ***p<0,001).

Results

The BMP4-BMPR1A axis is specifically dysregulated in BLBC and associated with poor prognostic.

Previously we demonstrated that the BMP pathway through the BMP2-BMPR1b axis, specifically deregulated in luminal tumors, was directly involved in early steps of MaSC transformation[36]. Given the enrichment of BLBCs in CSC and the involvement of the BMP pathway in the regulation of these cells[36] we tested whether the BMP pathway could also play a role in emergence of BLBCs. We focused our analyses on BMP4 previously showed to have a specific effect on BLBC cell lines as compared to luminal ones[40]. in addition, the BMPR1A receptor was described as overexpressed in BLBC as compared to normal mammary epithelium[41]. We first compared the transcriptional expression profile of BMPR1A, and BMP4 in the different breast cancer molecular subtypes and in normal breast tissue (TCGA-Breast cancer and GTEx cohorts). We observed a slight decrease of BMPR1A mRNA expression in all molecular subtypes of breast cancers when compared to healthy and peritumoral tissue (Figure 1A and Appendix Figure S1A). A marked decrease of BMP4 mRNA expression was specifically observed in basal-like tumors as compared to other breast cancer molecular subtypes as well as healthy and peritumoral tissue (Appendix Figure S1B). Interestingly, the amounts of soluble BMP4 ligand in BLBC and normal mammary gland were similar, suggesting that tumoral cells are not the main source of BMP4 within the tumor microenvironment (Appendix Figure S1C). As the BMPR1A mRNA levels were largely heterogenous between basal-like tumors (Figure 1A), we tested whether high or low levels of BMPR1A mRNA could be correlated to patients prognosis. Interestingly, high

BMPR1A expression was specifically associated with a poor prognosis in the basal-like subtype. In contrast, a faint but significant better prognosis is associated with high BMPR1A expression when considering all breast cancer molecular subtypes together (Figure 1B). Interestingly, in-silico analyses carried out on the TCGA breast cancer cohort showed that high BMPR1A expression was correlated with the expression of genes involved in chromatin remodeling, migration and response to DNA damage (Figure 1C). Given the inverse correlation between BMPR1A expression and BLBC patients survival and the key role of BRCA1 in this molecular subtype, we then evaluated the correlation between BMPR1A and BRCA1 expression. We selected BRCA1 wild-type triple-negative breast cancer tumors for which the membrane expression of basal cytokeratin 14 (CK14) was also assessed (Appendix Figure S2A), the latter being highly specific to basal-like breast cancers[42–44]. We then quantified BMPR1A protein expression by immunohistochemistry (Figure 1D) and BRCA1 mRNA expression by RT-qPCR. Univariate linear regression showed a significant inverse relationship between BRCA1 mRNA and BMPR1A protein levels (Figure 1E). Furthermore, bivariate linear regression models showed the persistence of this relationship after adjustment for age, stage and CK14 membrane expression respectively (Appendix Figure S2B). We then compared BMPR1A or BMP4 mRNA expression in healthy mammary epithelial cells from normal donors and from healthy donors' carriers of the germinal mutations in BRCA1 and therefore strongly predisposed to develop BLBC[45]. We observed here no significant differences in BMPR1A expression, (Figure 1F). Importantly, we observed a significant decrease in the expression of BMPR1B, the other type 1 BMP receptor. This indicates that in BRCA1 mutated but healthy mammary epithelial cells, the BMPR1A-mediated signaling is likely dominant (Figure 1G). In BRCA1-mutated healthy mammary cells, we observed a trend to a lower BMP4 expression as compared to wild-type samples (Appendix Figure S2C), however non-significant and not confirmed at the secreted protein level (Appendix Figure S2D. These data suggest that a alterations of the BMP pathway is associated with BRCA1 deficiency at a very early, pre-transformation stage. Collectively, these results, together with the previously detailed data, suggest that BMPR1A expression

is associated with poor prognosis and inversely correlated to BRCA1 transcriptional expression in basal-like breast cancers.

BMP4 induces a switch from luminal to myoepithelial differentiation through BRCA1 repression.

In order to evaluate and compare the relative importance of decrease of BRCA1 level and/or of the BMP4-BMPR1A signal, we analyze their impacts on the progenitors differentiation from MaSC using the epithelial Colonies forming cell assay (E-CFC)(Appendix Figure S3A). We then observed in healthy mammary epithelial cells isolated from BRCA1 haplo-insufficiency patients (BRCA1) that undergoes prophylactic mastectomy (high-risk patients) a significant increase in myoepithelial progenitors at the expense of the luminal ones when compared to epithelial cells from BRCA1 Wild-type (WT) healthy tissue (Figure 2A). This is consistent with the previously known role of BRCA1 in the luminal differentiation. Interestingly, a three days BMP4 treatment of MCF10A cells, a human immortalized but not transformed model of mammary stem cells and progenitors[46], induces a similar switch from luminal to myoepithelial progenitors' frequency while the total number of colony forming cells is only marginally decreased, suggesting that some luminal progenitors adopt a myoepithelial fate under BMP4 signaling (Figure 2B and Appendix Figure S3B). To determine if BRCA1 could play a role in luminal and myoepithelial progenitors fate choice in MCF10A cells, we developed a Doxycycline-inducible shBRCA1 model that we validated at the transcriptional and protein levels (Figure 2C and 2D). The repression of BRCA1 in MCF10A cells specifically induces an increase of myoepithelial progenitors frequency at the expense of luminal progenitors, similarly to BMP4 treatment (Figure 2E and Appendix Figure S3C). Interestingly, both BMP4 and BRCA1 knock-down also induced an increase in the frequency of mammosphere forming cells, showing an increase in the more immature cell fraction (Appendix Figure S3D and S3E). Together with the inverse correlation between BRCA1 transcript levels and BMPR1A, these data suggest a functional interaction between BRCA1 and BMP4 signaling. To test this hypothesis, we measured by qRT-PCR the specific effect of BRCA1 repression by shRNA in MCF10A cells on the expression of several genes involved in BMP4 signaling (BMP receptors; SMAD1, 5 and 8: effectors SMAD; SMAD4: co-SMAD of the BMP and TGF signaling). No significant

effect of BRCA1 knock-down was observed at the transcriptional level (Figure 2F). Similarly, RNA-seq data from wild-type of BRCA1-mutated healthy mammary gland showed that the expression of the same genes was not significatively changed in primary epithelial cells regardless of their BRCA1 genomic status (Figure 2G). We then evaluated if BMP4 signaling could impact BRCA1 expression. MCF10A cells that were exposed 48 hours to BMP4 displayed more than 50% repression of BRCA1 mRNA expression (Figure 2H, left panel) and primary transcript (Figure 2H, right panel) suggesting a BMP4-mediated BRCA1 transcriptional repression. Moreover, BRCA1 repression by BMP4 was also observed at protein level and was completely reversed by LDN-193189 (a preferential BMPR1A and BMP canonical pathway inhibitor) (Figure 2I). Altogether, these results indicate the involvement of these BMP signaling effectors in repressing BRCA1 level.

BMP4 induces aberrant RAD51 recruitment after DNA double-strand breaks

Two main pathways are described for DNA double-strand break repair: Homologous Recombination (HR) and Non-Homologous End Joining (NHEJ). Homologous recombination is a process based on the availability of uninjured homologous DNA from the sister chromatid. Its use is therefore restricted to the S and G2 phases of the cell cycle. However, it is an error-free repair pathway provided that the correct homologous sequence is used. This is a multi-step process involving not only BRCA1 but also numerous other effectors such as RAD51, which plays a major role in homologous strand search and invasion, a key step in the HR process[13]. RAD51 nuclear recruitment after DNA damage has been described as a marker of homologous recombination proficiency[47–51]. Conversely, NHEJ is an error-prone repair mechanism that can be evidenced by 53BP1 recruitment at the DSB[13]. We then assessed the impact of BMP4 exposure on the homologous recombination status in MCF10A cells. To do this, we measured by immunofluorescence the nuclear recruitment of RAD51 after irradiation. Additionally, we employed two complementary immunostains: γH2AX, serving as a marker for DNA double-strand breaks, and 53BP1, indicating activation of the NHEJ pathway. We first validated the suitability of this approach in MCF10A cells by using an inducible shBRCA1 model (Figure 2C & 2D).

Transcriptional BRCA1 repression by shRNA induction did not induce a significant difference in the number of double-strand breaks generated 1 hour after irradiation as compared to controls (Figure 3A). However, it did induce a drastic impairment of RAD51 recruitment (Figure 4B), thus validating the use of this functional approach in the MCF10A cell line. Surprisingly, after exogenous BMP4 exposure, we did not observe any deficiency in RAD51 nuclear recruitment but rather an aberrant RAD51 over-recruitment (Figure 3C). BMP4 treatment was not accompanied by an increase in γH2Ax foci (Figure 3D) nor in RAD51 protein level (Figure 3E). While RAD51 typically maintains genome integrity through homologous recombination, it is often overexpressed in unstable cancers like TNBC[52]. This overexpression may drive pathological recombination, causing chromosomal aberrations linked to carcinogenesis[53–60]. Notably, 53BP1 has been identified as an inhibitor of this tumorigenic process[61]. BMP4 exposure induced a major RAD51 (Figure 4F and 4G) and 53BP1 (Figure 4F and 4H) nuclear recruitment as compared to untreated cells that only induced a modest 53BP1 and RAD51 nuclear recruitment. Taken together, these data support the hypothesis that immature mammary cells have an altered HR in response to BMP4-mediated BRCA1 repression.

The BMP4-BMPR1A signaling induces an increased sensitivity to PARPi.

We then explored if the increased RAD51 and 53BP1 recruitment induced by BMP4 on DSB impact the functionality of the HR. PARP1 and PARP2 are enzymes that repair DNA single-strand breaks. PARP inhibitors (PARPi) block these enzymes, causing DSB accumulation. In homologous recombination-deficient cells, this leads to cell death by activating error-prone repair systems, a concept known as synthetic lethality[62,63]. PARP inhibitors are effective in treating certain cancers with homologous recombination deficiencies, such as specific ovarian and breast cancers with BRCA1/2 mutations[64–71]. Sensitivity to PARP inhibitors can therefore be used as a read out of HRD. As a control for our ability to detect HRD, we first measured the proliferation response of MCF10A cells in function of the PARPi (Olaparib) dose following shRNA mediated knock-down of BRCA1. As expected, cells bearing an inducible lentiviral vector with a shRNA directed against the Luciferase mRNA (as a control)

had similar sensitivity to Olaparib with or without doxycycline induction (Figure 4A). On the other hand, cells bearing an inducible lentiviral vector with a shRNA directed against the BRCA1 mRNA showed a significant increase in Olaparib sensitivity in presence of doxycycline (Figure 4A). When we performed the same assay using MCF10A cells exposed to BMP4 in the presence or not of the BMP inhibitor LDN-193189, we observed an increased sensitivity to Olaparib (Figure 4B and 4C) to the same extent than with a BRCA1 knock-down (Figure 4A). Importantly, this effect was fully reversed in the presence of LDN-193189. A similar effect was also found using another PARPi, talazoparib, eliminating a possible off-target effect of Olaparib and confirming a class effect of PARPis. Again, LDN-193189 completely reversed this effect suggesting the involvement of the BMP canonical pathway and more specifically of BMPR1A receptor in the PARPi sensitivity of BMP4-exposed MCF10A (Figure 4D). To test this hypothesis, we generated a BMPR1A-overexpressing MCF10A cell line (MCF10A-R1A+) that was validated at both transcriptional and protein levels as compared to MCF10A transduced with an empty vector (MCF10A-EV)(Figure 4E and 4F). BMPR1A over-expression, alone or in combination with BMP4 exposure, led to a similar increase in Olaparib sensitivity (Figure 4G). LDN-193189 reversed this effect, thus confirming the involvement of BMPR1A in these BMP4-mediated iPARP sensitivity.

Altogether these data suggest that BMP4, through its binding to BMPR1A, is able to modulate the functionality of the HR likely through BRCA1 repression.

BMP4 allow the persistence of a fraction of genetically unstable immature cells at risk of basal-like transformation.

Preclinical data for Olaparib initially tested on BRCA1-deficient embryonic stem cells showed that its antiproliferative effect was mediated by cell cycle arrest in G2/M followed by significant apoptosis[62]. We then evaluated the apoptosis and fate of cells showing reduced proliferation under BMP4 exposure after Olaparib treatment. BMP4 and Olaparib co-exposure induced a significant increase in apoptosis compared with controls (Figure 5A). To quantify more accurately the cytokine effect on the cell cycle state of the cells, the Fluorescent and Ubiquination-based Cell Cycle Indicator

(FUCCI)–[72–75] was incorporated into our models to generate the MCF10A-FUCCI. BMP4 and Olaparib co-exposure did not induce a significantly visible blockage in G2/M (Fig 5B). However, we observed a significant accumulation of cells in G0/early G1 as compared to untreated MCF10A cells, suggesting a slowing of the cell cycle in this condition (Fig 5B and Appendix Fig S4A). Interestingly, exposure to BMP4 or Olaparib alone also resulted in cell cycle slowing, but to a lesser extent. To test whether the accumulation of cells in G0/G1 is related to an immature phenotype, we quantified by mammosphere and E-CFC assays the stem cell/progenitor ratio in each experimental condition. We measured a significant higher MaSC/CFC ratio (over 6-folds) in surviving cells treated by BMP4 in combination to Olaparib and as compared to untreated cells or cells treated with BMP4 or Olaparib alone. These experiments then showed a strong increase in stemness in response to the Olaparib and BMP4 combination that was reversed by the LDN-193189 inhibitor (Fig 5C). The persistence of this stem-like cells with reduced BRCA1 expression levels and altered HR could lead to a genetic instability phenotype. To test this hypothesis, we evaluated the level of genetic stability of persistent cells after BMP4 exposure and Olaparib treatment by performing a neutral comet assay to identify unresolved DNA double-strand breaks and an alkaline comet assay to assess a broader spectrum of DNA damage, including single-strand breaks. We observed that in persistent cells, BMP4 and Olaparib co-exposure induced a significantly greater number of double-strand breaks (Figure 5D, 5E and Appendix Figure S4B). Finally, to test whether the accumulation of such DNA damage would be able to induce transformation of cells subjected to BMP4-BMPR1A signaling, we then exposed BMPR1A-overexpressing MCF10A cells and their control to BMP4 in a 18-week long-term exposure at the end of which we performed a soft agar assay. BMP4 exposure or BMPR1A overexpression generated a greater number of soft-agar colonies than in the control condition (Figure 5F-G), indicating that immature mammary cells spared in the presence of BMP4 under PARPi may display a certain degree of genetic instability under the influence of the BMP4/BMPR1A axis and lead to their transformation upon long-term exposure.

Discussion

Basal-like breast cancer presents significant clinical challenges due to its aggressive nature and limited targeted therapeutic options. A substantial proportion of these cancers are not associated with BRCA1 mutations, complicating treatment strategies and underscoring the need for alternative approaches. Poly (ADP-ribose) polymerase inhibitors (PARPi) have emerged as a promising therapeutic option, particularly in tumors with deficiencies in homologous recombination repair, offering a synthetic lethality approach to target these malignancies [79]. However, the persistence of cancer stem cells raises critical challenge to achieve a durable remission, as these cells are often resistant to therapies, including PARPi, and contribute to disease recurrence and metastasis[79]. In this context, our study provides a new insight into early mechanisms that could promote basal-like carcinogenesis in the absence of BRCA1 mutations. We revealed the role of the mammary gland microenvironment through a key role of the BMP4-BMPR1A axis. Analyses carried out on patient cohorts identified that, although BMP4 protein and its receptor BMPR1A mRNA are not differentially expressed in predisposed $BRCA1^{+/-}$ healthy mammary gland or BLBC, high BMPR1A expression at the mRNA level correlates to a poor prognosis specifically in BLBC. Moreover, for the first time, we show that BMPR1A protein expression is inversely correlated to BRCA1 mRNA expression and indicative of bad prognosis.

The effects of an activation of the BMP4/BMPR1A axis directly on MaSC and progenitors' population were conducted taking advantage of the MCF10A cell line, that is immortalized but not transformed (CDKN2A homozygous deletion, cMYC amplification)[80]. This cellular model also represents an heterogeneous population of human mammary stem-like cells able to generate bipotent or unipotent luminal and basal progenitors an responsive to microenvironmental cues[36]. We revealed that BMP4 induces a transcriptional repression of BRCA1, associated with and sufficient to induce a switch of MaSC fate towards basal progenitors' differentiation. Accordingly, we evidenced a role of BRCA1 repression on progenitors' fate in the mammary gland toward an enrichment in basal differentiation and stemness, mimicking what is known for BMP4 impact on human primary mammary

stem cells[36,81,82]. This is also consistent with several previous studies carried out *ex vivo* under BRCA1 haploinsufficiency[83–85] and in vitro[86,87] that all have highlighted the role of BRCA1 in differentiating luminal progenitors in the mammary gland. This is also according to the fact that BRCA1 has been showed to control luminal differentiation through the molecular interaction with GATA3 to repress FOXC1[88]. Importantly we have demonstrated that BMP2 and BMP4 distinctly controlled differentiation respectively toward luminal or myoepithelial/basal lineage[36,89]. Concerning luminal commitment inhibited by BMP4, we demonstrated that BMP2 control the expression of GATA3 to repress FOXC1[36,90] suggesting that it likely involves regulation of BRCA1 expression by BMPS. Therefore, for the first time, our data link basal differentiation mediated by BRCA1 repression upon the BMP signaling in non-transformed cells.

Poly (ADP-ribose) polymerase (PARP) 1 and PARP2 are enzymes involved in the response to DNA damage, in particular DNA single-strand break repair by base excision. PARP inhibitors (PARPi) are competitive inhibitors of PARP1 and PARP2. This results in the non-resolution of single-strand DNA breaks and the trapping of PARP enzymes on damaged DNA. The resulting blockage of the replication fork when the cell enters the replicative phase leads to the formation of DSBs. In the context of a homologous recombination deficiency, this damage of the replication fork cannot be reliably repaired. This leads to the activation of other error-prone repair systems favoring the accumulation of genetic aberrations leading to cell death by apoptosis in accordance with the principle of synthetic lethality[62,63]. PARP inhibitors therefore constitute a new therapeutic option which has demonstrated its efficacy in conditions of homologous recombination deficiency in several tumor locations, notably certain epithelial ovarian cancers and certain breast cancers with a constitutional BRCA1/2 deleterious mutation[64–71]. It is then of major importance that we demonstrated that the BRCA1 repression induced by BMP4 is sufficient to induce homologous recombination defects as evidenced by an increased sensitivity to PARPi. Moreover, while BMP4-induced HRD and Olaparib-induced DNA damage have an additive effect on apoptosis-induced cell death, our data also revealed an accumulation of surviving cells in a G0/G1 stage correlated with an increase of immaturity features. This preferential survival of

immature resting cells could constitute a cellular reservoir of preneoplastic cells. Indeed, comet assays further suggest an associated genomic instability due to BMP4-induced HRD and indicated by accumulation of unresolved DSB after PARPi treatment. The notion that only a partial decrease in BRCA1 function can induce a genomic instability that could lead to transformation is supported by other studies. For example, it has been demonstrated that the introduction of a heterozygous BRCA1 pathogenic mutation (185delAG) into the MCF10A cell line ($BRCA1^{mut/+}$) lead, upon SNP array and FISH evaluation, to significant copy number alterations compared with the $BRCA1^{+/+}$ control cell line[91]. In addition, non-transformed BRCA1 mutated tissues show a higher level of chromosomal aberrations in CGH than non-mutated control tissues (but less than BRCA1 mutated tumors)[92]. Finally, unlike BRCA-mutated ovarian tumors, complete loss of the BRCA1 WT allele is not necessarily required for the carcinogenesis of BRCA1-mutated breast tumors[93]. BRCA1 partial defect is thus sufficient to generate genetic instability at the pre-transformation stage and also transformation. Hyper-recombination phenomena associated with BRCA1 haploinsufficiency could be at the origin of this initial genetic instability[94]. Our results are therefore compatible with this hypothesis since, under BMP4 exposure, we observed aberrant nuclear RAD51 over-recruitment after MCF10A irradiation. Many authors have suggested that such RAD51 over-recruitment at the break site could be deleterious, promoting inappropriate non-homologous hyper-recombination and hence the emergence of chromosomal aberrations such as translocations, inversions or deletions leading to loss of heterozygosity and aneuploidy that may be involved in carcinogenesis[53–60]. Also, RAD51 is able to intrinsically generate genetic instability through non-homologous (or micro-homologous) recombination, and that this process is prevented by 53BP1[61].

In this context, we demonstrate here that chronic exposure to BMP4 signal could induce transformation. Indeed, long-term treatments of the MCF10A cell line with BMP4, showed that BMP4-induced BRCA1 repression is correlated to the induction of an transformed phenotype *in-vitro*. This uncovers a new mechanism to establish a BRCAness phenotype in non-transformed cells through a BMP4-BMPR1A mediated BRCA1 transcriptional repression.

Our results suggest that, in a physiological context, BMP4 is an important cytokine of the mammary gland microenvironment that induce the basal differentiation of the mammary progenitors[36], acting at least in part through BRCA1 repression. BMP4 signaling is likely integrated with other cytokines and hormones to ensure the homeostasis and plasticity of the mammary gland during life. BRCAness induced by germline BRCA1 mutations, albeit present in all cells of the body, predispose almost exclusively to cancers of the breast and ovary, two organs where female hormones play a key role. Among these hormones, estrogens and especially estradiol (E2) seems particularly interesting in this context. Indeed, E2 is involved in luminal differentiation and activates BRCA1 expression, therefore suggesting that BMP4 and E2 could control a balance between basal and luminal differentiation. Any alteration of this balance in favor of BMP4 signaling could lead to increased basal differentiation associated with a BRCA1 deficiency and genomic instability. Chronic exposure to environmental pollutants could be an example of perturbation since we previously showed that exposure to Bisphenol A or Benzo(A)pyrene, both associated to increased BC risk[95,96] strongly increase BMPR1A expression and affect stem cells features[89]. This study contributes to a better understanding of the complex regulatory mechanisms controlling mammary cell fate and BRCA1 expression.

In clinic, PARP inhibitors are used in subsets of BLBC patients with BRCA1 germline mutation but this could represent only a subset of BLBC patients that could benefit from therapies exploiting HRD. Identifying BLBC patients with ongoing HRD due to increased BMP4/BMPR1A signaling and subsequent BRCA1 repression could led to expand the successful use of PARP inhibitors. In addition, targeting the BMP4/BMPR1A pathway in these BLBC could be an alternative therapeutic option that should be further explored to benefit to treatment of patients with the most aggressive breast cancer subtype.

Ethic statement

The use of patient samples was validated by the ethical committee of the Centre Léon Bérard under treatment number R201-004-531. All patients previously gave their informed consent for the use of the samples.

Authors' Contributions

Simon AHO: Conceptualization, investigation, methodology, formal analysis, writing original draft. Marie PERBET : Investigation. Isabelle TREILLEUX : Formal analysis, investigation. Adrien BUISSON : Investigation. Sandrine JEANPIERRE : Investigation, methodology, Emmanuel DELAY : Conceptualization, supervision, resources. Véronique MAGUER-SATTA : Conceptualization, formal analysis, supervision, funding acquisition, investigation, methodology, writing original draft, project administration. Boris GUYOT: Conceptualization, formal analysis, supervision, funding acquisition, investigation, methodology, writing original draft.

Acknowledgments

We thank Dr Patrick Mehlen for its support and helpful advices. We thank P. Battiston-Montagne and C. Vanbelle, CRCL-PIC cytometry and imaging platform. This study was funded by Fondation ARC (V. Maguer-Satta and S.Aho,); Fondation pour la Recherche Médicale (EQU202203014695, V. Maguer-Satta) ; Association Déchaîne Ton Cœur (V. Maguer-Satta); Association RUBAN ROSE Prix Avenir 2021 (V. Maguer-Satta); Association « Sein Léman Avenir (S. Aho); Ligue 74 de Prévention du Cancer du Sein (V.Maguer-Satta and E.Delay).

Figures legends

Figure 1. BMPR1A mRNA expression in different breast cancer molecular subtypes, compared with healthy and peri-tumoral control tissues in the TCGA-Breast Cancer and GTEx cohorts (A). Kaplan Meier curves representing overall survival according to BMPR1A transcriptional expression in the TCGA cohort, among basal-like cancers (left panel) and all molecular subtypes (right panel) (B). Correlation

analysis related to BMPR1A transcriptional expression in the TCGA Breast Cancer cohort. Genes differentially expressed when comparing samples with high and low BMPR1A expression are classified into Gene Ontology functional groups. The level of statistical significance is plotted on the left, and the number of differentially expressed genes associated with each functional group is plotted on the right (C). Representative pictures of low and strong IHC staining of BMPR1A expression in TNBC. Magnification x20 (D). Univariate linear regression model showing the relationship between BRCA1 transcriptional expression (normalized on ACTB1 gene expression) and BMPR1A expression assessed according to a score defined by the percentage of positive cells x staining intensity following IHC staining (E). RT-qPCR analysis of BMPR1A transcriptional expression in healthy BRCA1 mutated tissues, compared to healthy wild-type control tissues. Error bars represent standard error to the mean (F). As in F for BMPR1B transcriptional expression (G).

Figure 2. Percentage of colonies formed in the E-CFC assay in non-transformed BRCA1 mutated mammary epithelial cells (BRCA1) compared with healthy unmutated control tissue (WT) (A). Percentage of colonies formed in the E-CFC assay on MCF10A cells exposed or not to BMP4 (20 ng/ml) for 72 hours (B). RT-qPCR analysis of BRCA1 mRNA level after shBRCA1 induction in the MCF10A cell line, normalized to the control shRNA targeting the luciferase mRNA (C). Western blot analysis of BRCA1 protein expression after shBRCA1 induction in the MCF10A cell line, normalized to the control shRNA targeting the luciferase mRNA (left panel). A representative western-blot picture is shown on the right (D). Specific effect of inducible shRNA-mediated BRCA1 knock-down in MCF10A cells on the expression of genes of the BMP pathway measured by RT-qPCR (F). RNAseq normalized counts of the indicated genes of the BMP patway in WT or BRCA1-mutated primary mammary epithelial cells (G). RT-qPCR analysis of BRCA1 mRNA (left panel) and primary transcript (right panel) expression in MCF10A cells exposed for 48 h to BMP4 (10 and 50 ng/ml) (H). Quantification and representative picture of western-blot analysis of BRCA1 protein expression in response to 48 h exposure to BMP4 (10 ng/ml) +/- LDN-193189 (100 ng/ml) added 2 h before BMP4. (I). Error bars represent standard error to the mean. *$p<0.05$, **$p<0.01$, ***$p<0.001$,****$p<0.0001$.

Figure 3. Immunofluorescence showing the number of γH2Ax foci formed 1 hour after a 2 Gy irradiation of MCF10A shBRCA1 and shluc cells with or without doxycycline induction. The left-hand picture is taken with a ZEISS epifluorescence microscope at x100 magnification. The right-hand graph is a quantification of the γH2Ax foci number per condition (A). Immunofluorescence showing the number of RAD51 foci formed 1 hour after a 2 Gy irradiation of MCF10A shBRCA1 and shLuc cells with or without doxycycline induction. The left-hand picture is taken with a ZEISS epifluorescence microscope at x100 magnification. The right-hand graph is a quantification of the γH2Ax foci number per condition (B). Immunofluorescence showing the number of RAD51 foci formed 1 hour after a 2 Gy irradiation of MCF10A cells pre-exposed or not to BMP4 (20 ng/ml). The left-hand picture is taken with a ZEISS epifluorescence microscope at x100 magnification. The right-hand graph is a quantification of the RAD51 foci number per condition (C). Quantification of the γH2Ax foci number formed 1 hour after a 2 Gy irradiation of MCF10A cells pre-exposed or not to BMP4 (20 ng/ml) (D). Representative picture and quantification of western-blot analysis of RAD 51 protein expression 1 hour after a 2 Gy irradiation of MCF10A cells pre-exposed or not to BMP4 (20 ng/ml) (E). Immunofluorescence showing the number of RAD51 and 53BP1 foci formed 1 hour, 4 hours, 10 hours and 24 hours after a 2 Gy irradiation of MCF10A cells pre-exposed or not to BMP4 (20 ng/ml). The top pictures are taken with a ZEISS epifluorescence microscope at x100 magnification at different post-irradiation time points. Quantification of RAD51 foci from F (G). Quantification of 53BP1 foci from F (H).

Figure 4. Proliferation assay of MCF10A cells with and without induction of shBRCA1 or shLuc and exposed for 7 days to various concentrations of Olaparib. Representative pictures of the cell culture at the end of the experiment are shown on the right and IC50 estimates with confidence intervals below (A). Proliferation assay of MCF10A cells exposed or not to BMP4 (20 ng/ml) or BMP4+LDN-193189 (100 ng/ml) and treated for 7 days with increasing doses of Olaparib. Representation as in A. (B). Clonogenic assay of MCF10A cells exposed or not to BMP4 (20ng/ml) or BMP4+LDN-193189 (100 ng/ml) and treated for 7 days with increasing doses of Olaparib (C). Proliferation assay of MCF10A cells exposed or not to BMP4 (20ng/ml) or BMP4+LDN-193189 (100 ng/ml) and treated for 7 days with increasing

doses of Talazoparib (D). BMPR1A mRNA level in BMPR1A-overexpressing MCF10A (MCF10A-R1A^{+}) compared with empty-vector control cells (MCF10A-EV) (E). Flow-cytometry analysis of membrane BMPRIA protein expression as in E (F). IC50 of Talazoparib in BMPR1A-overexpressing MCF10A cells or the empty-vector control cells, exposed or not to BMP4 (20ng/ml) and LDN-193189 (100 ng/ml) and treated for 7 days with increasing doses of Olaparib (G). Error bars represent standard error to the mean and all IC50 estimates were generated using a 4-parameter Weibull model.

Figure 5. Quantification and representative picture of western blot analysis of cleaved caspase-3 protein expression in MCF10A cells exposed or not to BMP4 (20ng/ml) or BMP4+LDN-193189 (100 ng/ml) and treated or not with Olaparib (0.75 μM) for 7 days. GAPDH was used as a loading control (A). Flow cytometry analysis in MCF10A-Fucci cells of the distribution in the different phases of the cell cycle of after exposure or not to BMP4 (20ng/ml) or BMP4+LDN-193189 (100 ng/ml) and treated or not with Olaparib (0.75 μM) for 7 days (B). Ratio between the number of stem cells (estimated using a mammospheres assay) and the number of progenitors (estimated using an E-CFC assay) in MCF10A cells exposed or not to BMP4 (20ng/ml) or BMP4+LDN-193189 (100 ng/ml) and treated or not with Olaparib (0.75 μM) for 7 days (C). Representative pictures of a neutral comet assay on MCF10A cells exposed or not to BMP4 (20ng/ml) or/and Olaparib (0.75 μM) after 7 days of treatment (D). Quantification of the olive moment in the Comet assay shown in D (E). Representative pictures of colonies (magnification: 10x) (F) and quantification (G) of the number of colonies formed in a soft-agar culture by MCF10A cells overexpressing or not BMPR1A and exposed or not to BMP4 for 20 weeks. Error bars represent standard error to mean. *$p<0.05$, **$p<0.01$, ***$p<0.001$,****$p<0.0001$.

References

1. Perou CM, Sørlie T, Eisen MB, et al. Molecular portraits of human breast tumours. *Nature*. 2000;406(6797):747-752. doi:10.1038/35021093

2. Sørlie T, Perou CM, Tibshirani R, et al. Gene expression patterns of breast carcinomas distinguish tumor subclasses with clinical implications. *Proc Natl Acad Sci USA*. 2001;98(19):10869-10874. doi:10.1073/pnas.191367098

3. Sørlie T, Tibshirani R, Parker J, et al. Repeated observation of breast tumor subtypes in independent gene expression data sets. *Proc Natl Acad Sci USA*. 2003;100(14):8418-8423. doi:10.1073/pnas.0932692100

4. Carey LA, Perou CM, Livasy CA, et al. Race, Breast Cancer Subtypes, and Survival in the Carolina Breast Cancer Study.

5. Millikan RC, Newman B, Tse CK, et al. Epidemiology of basal-like breast cancer. Published online 2008.

6. Fan C, Weigelt B. Concordance among Gene-Expression–Based Predictors for Breast Cancer. *n engl j med*. Published online 2006.

7. Banerjee S. Basal-like breast carcinomas: clinical outcome and response to chemotherapy. *Journal of Clinical Pathology*. 2006;59(7):729-735. doi:10.1136/jcp.2005.033043

8. Carey LA, Dees EC, Sawyer L, et al. The Triple Negative Paradox: Primary Tumor Chemosensitivity of Breast Cancer Subtypes. *Clinical Cancer Research*. 2007;13(8):2329-2334. doi:10.1158/1078-0432.CCR-06-1109

9. Parker JS, Mullins M, Cheang MCU, et al. Supervised Risk Predictor of Breast Cancer Based on Intrinsic Subtypes. *JCO*. 2009;27(8):1160-1167. doi:10.1200/JCO.2008.18.1370

10. Nguyen QH, Pervolarakis N, Blake K, et al. Profiling human breast epithelial cells using single cell RNA sequencing identifies cell diversity. *Nat Commun*. 2018;9(1):2028. doi:10.1038/s41467-018-04334-1

11. Rouzier R, Perou CM, Symmans WF, et al. Breast Cancer Molecular Subtypes Respond Differently to Preoperative Chemotherapy. *Clinical Cancer Research*. 2005;11(16):5678-5685. doi:10.1158/1078-0432.CCR-04-2421

12. Manié E, Popova T, Battistella A, et al. Genomic hallmarks of homologous recombination deficiency in invasive breast carcinomas: Genomic hallmarks of homologous recombination defect. *Int J Cancer*. 2016;138(4):891-900. doi:10.1002/ijc.29829

13. Scully R, Panday A, Elango R, Willis NA. DNA double-strand break repair-pathway choice in somatic mammalian cells. *Nat Rev Mol Cell Biol*. 2019;20(11):698-714. doi:10.1038/s41580-019-0152-0

14. Paul A. The breast cancer susceptibility genes (BRCA) in breast and ovarian cancers. *Front Biosci*. 2014;19(4):605. doi:10.2741/4230

15. Lord CJ, Ashworth A. BRCAness revisited. *Nat Rev Cancer*. 2016;16(2):110-120. doi:10.1038/nrc.2015.21

16. Staaf J, Glodzik D, Bosch A, et al. Whole-genome sequencing of triple-negative breast cancers in a population-based clinical study. *Nat Med*. 2019;25(10):1526-1533. doi:10.1038/s41591-019-0582-4

17. Severson TM, Wolf DM, Yau C, et al. The BRCA1ness signature is associated significantly with response to PARP inhibitor treatment versus control in the I-SPY 2 randomized neoadjuvant setting. *Breast Cancer Res*. 2017;19(1):99. doi:10.1186/s13058-017-0861-2

18. Chopra N, Tovey H, Pearson A, et al. Homologous recombination DNA repair deficiency and PARP inhibition activity in primary triple negative breast cancer. *Nat Commun*. 2020;11(1):2662. doi:10.1038/s41467-020-16142-7

19. The Cancer Genome Atlas Network. Comprehensive molecular portraits of human breast tumours. *Nature*. 2012;490(7418):61-70. doi:10.1038/nature11412

20. Turner NC, Reis-Filho JS, Russell AM, et al. BRCA1 dysfunction in sporadic basal-like breast cancer. *Oncogene*. 2007;26(14):2126-2132. doi:10.1038/sj.onc.1210014

21. Joosse SA, van Beers EH, Tielen IHG, et al. Prediction of BRCA1-association in hereditary non-BRCA1/2 breast carcinomas with array-CGH. *Breast Cancer Res Treat*. 2009;116(3):479-489. doi:10.1007/s10549-008-0117-z

22. Junankar S, Baker LA, Roden DL, et al. ID4 controls mammary stem cells and marks breast cancers with a stem cell-like phenotype. *Nat Commun*. 2015;6(1):6548. doi:10.1038/ncomms7548

23. Garcia AI, Buisson M, Bertrand P, et al. Down-regulation of *BRCA1* expression by miR-146a and miR-146b-5p in triple negative sporadic breast cancers. *EMBO Mol Med*. 2011;3(5):279-290. doi:10.1002/emmm.201100136

24. Fkih M'hamed I, Privat M, Ponelle F, Penault-Llorca F, Kenani A, Bignon YJ. Identification of miR-10b, miR-26a, miR-146a and miR-153 as potential triple-negative breast cancer biomarkers. *Cell Oncol*. 2015;38(6):433-442. doi:10.1007/s13402-015-0239-3

25. Moskwa P, Buffa FM, Pan Y, et al. miR-182-Mediated Downregulation of BRCA1 Impacts DNA Repair and Sensitivity to PARP Inhibitors. *Molecular Cell*. 2011;41(2):210-220. doi:10.1016/j.molcel.2010.12.005

26. Shen J, Ambrosone CB, Zhao H. Novel genetic variants in microRNA genes and familial breast cancer. *Int J Cancer*. 2009;124(5):1178-1182. doi:10.1002/ijc.24008

27. De Summa S, Pinto R, Pilato B, et al. Expression of base excision repair key factors and miR17 in familial and sporadic breast cancer. *Cell Death Dis*. 2014;5(2):e1076-e1076. doi:10.1038/cddis.2014.30

28. Liu L, Zhou W, Cheng CT, et al. TGFβ Induces "BRCAness" and Sensitivity to PARP Inhibition in Breast Cancer by Regulating DNA-Repair Genes. *Molecular Cancer Research*. 2014;12(11):1597-1609. doi:10.1158/1541-7786.MCR-14-0201

29. Pal D, Pertot A, Shirole NH, et al. TGF-β reduces DNA ds-break repair mechanisms to heighten genetic diversity and adaptability of CD44+/CD24− cancer cells. *eLife*. 2017;6:e21615. doi:10.7554/eLife.21615

30. Nielsen TO, Hsu FD, Jensen K, et al. Immunohistochemical and Clinical Characterization of the Basal-Like Subtype of Invasive Breast Carcinoma. *Clinical Cancer Research*. 2004;10(16):5367-5374. doi:10.1158/1078-0432.CCR-04-0220

31. Livasy CA, Karaca G, Nanda R, et al. Phenotypic evaluation of the basal-like subtype of invasive breast carcinoma. *Modern Pathology*. 2006;19(2):264-271. doi:10.1038/modpathol.3800528

32. Honeth G, Bendahl PO, Ringnér M, et al. The CD44+/CD24-phenotype is enriched in basal-like breast tumors. *Breast Cancer Res*. 2008;10(3):R53. doi:10.1186/bcr2108

33. Conde I, Ribeiro AS, Paredes J. Breast Cancer Stem Cell Membrane Biomarkers: Therapy Targeting and Clinical Implications. *Cells*. 2022;11(6):934. doi:10.3390/cells11060934

34. Molyneux G, Geyer FC, Magnay FA, et al. BRCA1 Basal-like Breast Cancers Originate from Luminal Epithelial Progenitors and Not from Basal Stem Cells. *Cell Stem Cell*. 2010;7(3):403-417. doi:10.1016/j.stem.2010.07.010

35. McMullen JRW, Soto U. Newly identified breast luminal progenitor and gestational stem cell populations likely give rise to HER2-overexpressing and basal-like breast cancers. *Discov Oncol*. 2022;13(1):38. doi:10.1007/s12672-022-00500-6

36. Chapellier M, Bachelard-Cascales E, Schmidt X, et al. Disequilibrium of BMP2 Levels in the Breast Stem Cell Niche Launches Epithelial Transformation by Overamplifying BMPR1B Cell Response. *Stem Cell Reports*. 2015;4(2):239-254. doi:10.1016/j.stemcr.2014.12.007

37. Bachelard-Cascales E, Chapellier M, Delay E, et al. The CD10 Enzyme Is a Key Player to Identify and Regulate Human Mammary Stem Cells. *Stem Cells*. 2010;28(6):1081-1088. doi:10.1002/stem.435

38. Akiyama T, Raftery LA, Wharton KA. Bone morphogenetic protein signaling: the pathway and its regulation. Treisman J, ed. *GENETICS*. 2024;226(2):iyad200. doi:10.1093/genetics/iyad200

39. Zabkiewicz C, Resaul J, Hargest R, Jiang WG, Ye L. Bone morphogenetic proteins, breast cancer, and bone metastases: striking the right balance. *Endocrine-Related Cancer*. 2017;24(10):R349-R366. doi:10.1530/ERC-17-0139

40. Sharma R, Gogoi G, Saikia S, et al. BMP4 enhances anoikis resistance and chemoresistance of breast cancer cells through canonical BMP signaling. *J Cell Commun Signal*. 2022;16(2):191-205. doi:10.1007/s12079-021-00649-9

41. Balboni AL, Hutchinson JA, DeCastro AJ, et al. ΔNp63α-mediated activation of bone morphogenetic protein signaling governs stem cell activity and plasticity in normal and malignant mammary epithelial cells. *Cancer Res*. 2013;73(2):1020-1030. doi:10.1158/0008-5472.CAN-12-2862

42. Botti G, Cantile M, Collina F, et al. Morphological and pathological features of basal-like breast cancer. *Transl Cancer Res*. 2019;8(S5):S503-S509. doi:10.21037/tcr.2019.06.50

43. Sousa B, Paredes J, Milanezi F, et al. P-cadherin, vimentin and CK14 for identification of basal-like phenotype in breast carcinomas: an immunohistochemical study. *Histol Histopathol*. 2010;25(8):963-974. doi:10.14670/HH-25.963

44. Thike AA, Cheok PY, Jara-Lazaro AR, Tan B, Tan P, Tan PH. Triple-negative breast cancer: clinicopathological characteristics and relationship with basal-like breast cancer. *Modern Pathology*. 2010;23(1):123-133. doi:10.1038/modpathol.2009.145

45. Futreal PA, Liu Q, Shattuck-Eidens D, et al. *BRCA1* Mutations in Primary Breast and Ovarian Carcinomas. *Science*. 1994;266(5182):120-122. doi:10.1126/science.7939630

46. Guyot B, Clément F, Drouet Y, et al. An Early Neoplasia Index (ENI10), Based on Molecular Identity of CD10 Cells and Associated Stemness Biomarkers, is a Predictor of Patient Outcome in Many Cancers. *Cancer Res Commun*. 2023;3(9):1966-1980. doi:10.1158/2767-9764.CRC-23-0196

47. Willers H, Taghian AG, Luo CM, Treszezamsky A, Sgroi DC, Powell SN. Utility of DNA Repair Protein Foci for the Detection of Putative BRCA1 Pathway Defects in Breast Cancer Biopsies. *Molecular Cancer Research*. 2009;7(8):1304-1309. doi:10.1158/1541-7786.MCR-09-0149

48. Naipal KAT, Verkaik NS, Ameziane N, et al. Functional *Ex Vivo* Assay to Select Homologous Recombination–Deficient Breast Tumors for PARP Inhibitor Treatment. *Clinical Cancer Research*. 2014;20(18):4816-4826. doi:10.1158/1078-0432.CCR-14-0571

49. Meijer TG, Verkaik NS, Sieuwerts AM, et al. Functional *Ex Vivo* Assay Reveals Homologous Recombination Deficiency in Breast Cancer Beyond BRCA Gene Defects. *Clinical Cancer Research*. 2018;24(24):6277-6287. doi:10.1158/1078-0432.CCR-18-0063

50. Castroviejo-Bermejo M, Cruz C, Llop-Guevara A, et al. A RAD 51 assay feasible in routine tumor samples calls PARP inhibitor response beyond BRCA mutation. *EMBO Mol Med*. 2018;10(12). doi:10.15252/emmm.201809172

51. Cruz C, Castroviejo-Bermejo M, Gutiérrez-Enríquez S, et al. RAD51 foci as a functional biomarker of homologous recombination repair and PARP inhibitor resistance in germline BRCA-mutated breast cancer. *Annals of Oncology*. 2018;29(5):1203-1210. doi:10.1093/annonc/mdy099

52. Wiegmans AP, Al-Ejeh F, Chee N, et al. Rad51 supports triple negative breast cancer metastasis. *Oncotarget*. 2014;5(10):3261-3272. doi:10.18632/oncotarget.1923

53. Kim PM. Overexpression of human RAD51 and RAD52 reduces double-strand break-induced homologous recombination in mammalian cells. *Nucleic Acids Research*. 2001;29(21):4352-4360. doi:10.1093/nar/29.21.4352

54. Worrillow LJ, Allan JM. Deregulation of homologous recombination DNA repair in alkylating agent-treated stem cell clones: a possible role in the aetiology of chemotherapy-induced leukaemia. *Oncogene*. 2006;25(12):1709-1720. doi:10.1038/sj.onc.1209208

55. Richardson C, Stark JM, Ommundsen M, Jasin M. Rad51 overexpression promotes alternative double-strand break repair pathways and genome instability. *Oncogene*. 2004;23(2):546-553. doi:10.1038/sj.onc.1207098

56. Martin RW, Orelli BJ, Yamazoe M, Minn AJ, Takeda S, Bishop DK. RAD51 Up-regulation Bypasses *BRCA1* Function and Is a Common Feature of *BRCA1* -Deficient Breast Tumors. *Cancer Research*. 2007;67(20):9658-9665. doi:10.1158/0008-5472.CAN-07-0290

57. Francis R, Richardson C. Multipotent hematopoietic cells susceptible to alternative double-strand break repair pathways that promote genome rearrangements. *Genes Dev*. 2007;21(9):1064-1074. doi:10.1101/gad.1522807

58. Klein HL. The consequences of Rad51 overexpression for normal and tumor cells. *DNA Repair*. 2008;7(5):686-693. doi:10.1016/j.dnarep.2007.12.008

59. Elango R, Sheng Z, Jackson J, et al. Break-induced replication promotes formation of lethal joint molecules dissolved by Srs2. *Nat Commun*. 2017;8(1):1790. doi:10.1038/s41467-017-01987-2

60. Marsden CG, Jensen RB, Zagelbaum J, et al. The Tumor-Associated Variant RAD51 G151D Induces a Hyper-Recombination Phenotype. Maizels N, ed. *PLoS Genet*. 2016;12(8):e1006208. doi:10.1371/journal.pgen.1006208

61. Guirouilh-Barbat J, Yu W, Babin L, et al. *RAD51 Promotes Non-Homologous Genetic Rearrangements That Are Prevented by 53BP1*. Molecular Biology; 2019. doi:10.1101/768788

62. Farmer H, McCabe N, Lord CJ, et al. Targeting the DNA repair defect in BRCA mutant cells as a therapeutic strategy. *Nature*. 2005;434(7035):917-921. doi:10.1038/nature03445

63. Bryant HE, Schultz N, Thomas HD, et al. Specific killing of BRCA2-deficient tumours with inhibitors of poly(ADP-ribose) polymerase. 2005;434.

64. de Bono J, Mateo J, Fizazi K, et al. Olaparib for Metastatic Castration-Resistant Prostate Cancer. *N Engl J Med*. 2020;382(22):2091-2102. doi:10.1056/NEJMoa1911440

65. Golan T, Hammel P, Reni M, et al. Maintenance Olaparib for Germline *BRCA* -Mutated Metastatic Pancreatic Cancer. *N Engl J Med*. 2019;381(4):317-327. doi:10.1056/NEJMoa1903387

66. Ray-Coquard I, Pautier P, Pignata S, et al. Olaparib plus Bevacizumab as First-Line Maintenance in Ovarian Cancer. *N Engl J Med*. 2019;381(25):2416-2428. doi:10.1056/NEJMoa1911361

67. Coleman RL, Fleming GF, Brady MF, et al. Veliparib with First-Line Chemotherapy and as Maintenance Therapy in Ovarian Cancer. *N Engl J Med*. 2019;381(25):2403-2415. doi:10.1056/NEJMoa1909707

68. González-Martín A, Pothuri B, Vergote I, et al. Niraparib in Patients with Newly Diagnosed Advanced Ovarian Cancer. *N Engl J Med*. 2019;381(25):2391-2402. doi:10.1056/NEJMoa1910962

69. Tutt ANJ, Garber JE, Kaufman B, et al. Adjuvant Olaparib for Patients with *BRCA1* - or *BRCA2* -Mutated Breast Cancer. *N Engl J Med*. 2021;384(25):2394-2405. doi:10.1056/NEJMoa2105215

70. Robson M, Im SA, Senkus E, et al. Olaparib for Metastatic Breast Cancer in Patients with a Germline *BRCA* Mutation. *N Engl J Med*. 2017;377(6):523-533. doi:10.1056/NEJMoa1706450

71. Litton JK, Rugo HS, Ettl J, et al. Talazoparib in Patients with Advanced Breast Cancer and a Germline *BRCA* Mutation. *N Engl J Med*. 2018;379(8):753-763. doi:10.1056/NEJMoa1802905

72. Cuitiño MC, Pécot T, Sun D, et al. Two Distinct E2F Transcriptional Modules Drive Cell Cycles and Differentiation. *Cell Reports*. 2019;27(12):3547-3560.e5. doi:10.1016/j.celrep.2019.05.004

73. Sakaue-Sawano A, Yo M, Komatsu N, et al. Genetically Encoded Tools for Optical Dissection of the Mammalian Cell Cycle. *Molecular Cell*. 2017;68(3):626-640.e5. doi:10.1016/j.molcel.2017.10.001

74. Tomura M, Sakaue-Sawano A, Mori Y, et al. Contrasting Quiescent G0 Phase with Mitotic Cell Cycling in the Mouse Immune System. Villunger A, ed. *PLoS ONE*. 2013;8(9):e73801. doi:10.1371/journal.pone.0073801

75. Zielke N, Edgar BA. FUCCI sensors: powerful new tools for analysis of cell proliferation: FUCCI sensors. *WIREs Dev Biol*. 2015;4(5):469-487. doi:10.1002/wdev.189

76. Creighton CJ, Li X, Landis M, et al. Residual breast cancers after conventional therapy display mesenchymal as well as tumor-initiating features. *Proc Natl Acad Sci USA*. 2009;106(33):13820-13825. doi:10.1073/pnas.0905718106

77. Lee HE, Kim JH, Kim YJ, et al. An increase in cancer stem cell population after primary systemic therapy is a poor prognostic factor in breast cancer. *Br J Cancer*. 2011;104(11):1730-1738. doi:10.1038/bjc.2011.159

78. Kabraji S, Solé X, Huang Y, et al. AKT1low quiescent cancer cells persist after neoadjuvant chemotherapy in triple negative breast cancer. *Breast Cancer Res*. 2017;19(1):88. doi:10.1186/s13058-017-0877-7

79. Kumar N, Ehsan S, Banerjee S, et al. The unique risk factor profile of triple-negative breast cancer: a comprehensive meta-analysis. *JNCI: Journal of the National Cancer Institute*. 2024;116(8):1210-1219. doi:10.1093/jnci/djae056

80. Soule HD, Maloney TM, Wolman SR, et al. Isolation and characterization of a spontaneously immortalized human breast epithelial cell line, MCF-10. *Cancer Res*. 1990;50(18):6075-6086.

81. Ketolainen JM, Alarmo EL, Tuominen VJ, Kallioniemi A. Parallel inhibition of cell growth and induction of cell migration and invasion in breast cancer cells by bone morphogenetic protein 4. *Breast Cancer Res Treat*. 2010;124(2):377-386. doi:10.1007/s10549-010-0808-0

82. Montesano R, Sarközi R, Schramek H. Bone morphogenetic protein-4 strongly potentiates growth factor-induced proliferation of mammary epithelial cells. *Biochem Biophys Res Commun*. 2008;374(1):164-168. doi:10.1016/j.bbrc.2008.07.007

83. kConFab, Lim E, Vaillant F, et al. Aberrant luminal progenitors as the candidate target population for basal tumor development in BRCA1 mutation carriers. *Nat Med*. 2009;15(8):907-913. doi:10.1038/nm.2000

84. Liu S, Ginestier C, Charafe-Jauffret E, et al. BRCA1 regulates human mammary stem/progenitor cell fate. *Proc Natl Acad Sci USA*. 2008;105(5):1680-1685. doi:10.1073/pnas.0711613105

85. Proia TA, Keller PJ, Gupta PB, et al. Genetic Predisposition Directs Breast Cancer Phenotype by Dictating Progenitor Cell Fate. *Cell Stem Cell*. 2011;8(2):149-163. doi:10.1016/j.stem.2010.12.007

86. Furuta S, Jiang X, Gu B, Cheng E, Chen PL, Lee WH. Depletion of BRCA1 impairs differentiation but enhances proliferation of mammary epithelial cells. *Proc Natl Acad Sci USA*. 2005;102(26):9176-9181. doi:10.1073/pnas.0503793102

87. He Z, Ghorayeb R, Tan S, et al. Pathogenic BRCA1 variants disrupt PLK1-regulation of mitotic spindle orientation. *Nat Commun*. 2022;13(1):2200. doi:10.1038/s41467-022-29885-2

88. Tkocz D, Crawford NT, Buckley NE, et al. BRCA1 and GATA3 corepress FOXC1 to inhibit the pathogenesis of basal-like breast cancers. *Oncogene*. 2012;31(32):3667-3678. doi:10.1038/onc.2011.531

89. Clément F, Xu X, Donini CF, et al. Long-term exposure to bisphenol A or benzo(a)pyrene alters the fate of human mammary epithelial stem cells in response to BMP2 and BMP4, by pre-activating BMP signaling. *Cell Death Differ*. 2017;24(1):155-166. doi:10.1038/cdd.2016.107

90. Forsman CL, Ng BC, Heinze RK, et al. BMP-binding protein twisted gastrulation is required in mammary gland epithelium for normal ductal elongation and myoepithelial compartmentalization. *Dev Biol*. 2013;373(1):95-106. doi:10.1016/j.ydbio.2012.10.007

91. Konishi H, Mohseni M, Tamaki A, et al. Mutation of a single allele of the cancer susceptibility gene *BRCA1* leads to genomic instability in human breast epithelial cells. *Proc Natl Acad Sci USA*. 2011;108(43):17773-17778. doi:10.1073/pnas.1110969108

92. Rennstam K, Ringberg A, Cunliffe HE, Olsson H, Landberg G, Hedenfalk I. Genomic alterations in histopathologically normal breast tissue from *BRCA1* mutation carriers may be caused by BRCA1 haploinsufficiency. *Genes Chromosom Cancer*. 2010;49(1):78-90. doi:10.1002/gcc.20723

93. King TA, Li W, Brogi E, et al. Heterogenic Loss of the Wild-Type BRCA Allele in Human Breast Tumorigenesis. *Ann Surg Oncol*. 2007;14(9):2510-2518. doi:10.1245/s10434-007-9372-1

94. Cousineau I, Belmaaza A. BRCA1 Haploinsufficiency, but not Heterozygosity for a BRCA1-truncating Mutation, Deregulates Homologous Recombination. *Cell Cycle*. 2007;6(8):962-971. doi:10.4161/cc.6.8.4105

95. Weber Lozada K, Keri RA. Bisphenol A increases mammary cancer risk in two distinct mouse models of breast cancer. *Biol Reprod*. 2011;85(3):490-497. doi:10.1095/biolreprod.110.090431

96. Amadou A, Praud D, Coudon T, et al. Risk of breast cancer associated with long-term exposure to benzo[a]pyrene (BaP) air pollution: Evidence from the French E3N cohort study. *Environ Int*. 2021;149:106399. doi:10.1016/j.envint.2021.106399

97. Chapellier M, Bachelard-Cascales E, Schmidt X, et al. Disequilibrium of BMP2 Levels in the Breast Stem Cell Niche Launches Epithelial Transformation by Overamplifying BMPR1B Cell Response. *Stem Cell Reports*. 2015;4(2):239-254. doi:10/ggcvt7

98. Clément F, Xu X, Donini CF, et al. Long-term exposure to bisphenol A or benzo(a)pyrene alters the fate of human mammary epithelial stem cells in response to BMP2 and BMP4, by pre-activating BMP signaling. *Cell Death & Differentiation*. 2017;24(1):155-166. doi:10/f9kbfc

Figure 1

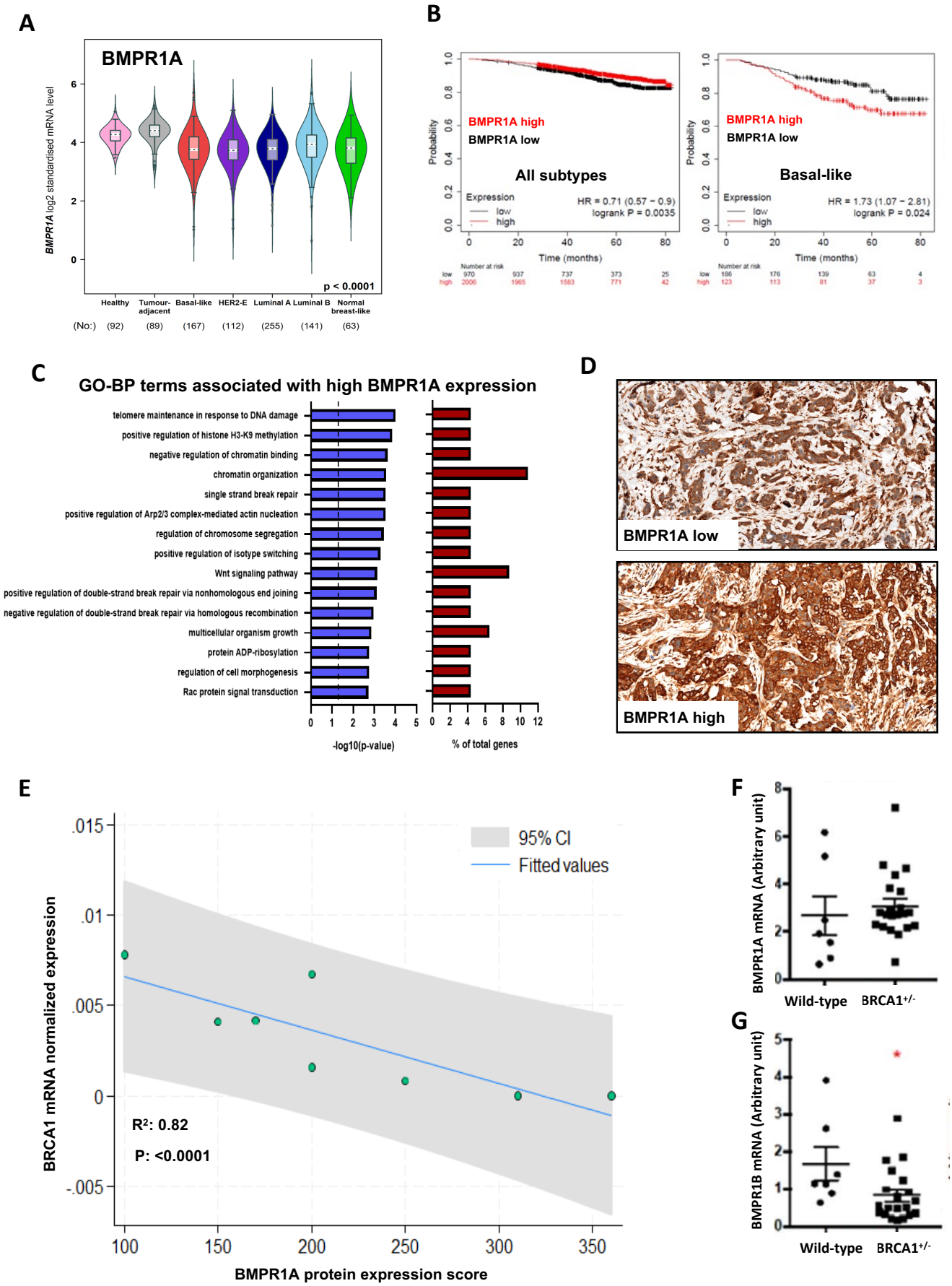
A
BMPR1A
BMPR1A log2 standardised mRNA level
p < 0.0001
Healthy
Tumour-adjacent
Basal-like
HER2-E
Luminal A
Luminal B
Normal breast-like
(No:) (92) (89) (167) (112) (255) (141) (63)
B
BMPR1A high
BMPR1A low
All subtypes
Expression
low
high
HR = 0.71 (0.57 − 0.9)
logrank P = 0.0035
Probability
Time (months)
Number at risk
low 970 937 737 373 25
high 2006 1965 1583 771 42
BMPR1A high
BMPR1A low
Basal-like
HR = 1.73 (1.07 − 2.81)
logrank P = 0.024
low 186 176 139 63 4
high 123 113 81 37 3
C
GO-BP terms associated with high BMPR1A expression
telomere maintenance in response to DNA damage
positive regulation of histone H3-K9 methylation
negative regulation of chromatin binding
chromatin organization
single strand break repair
positive regulation of Arp2/3 complex-mediated actin nucleation
regulation of chromosome segregation
positive regulation of isotype switching
Wnt signaling pathway
positive regulation of double-strand break repair via nonhomologous end joining
negative regulation of double-strand break repair via homologous recombination
multicellular organism growth
protein ADP-ribosylation
regulation of cell morphogenesis
Rac protein signal transduction
-log10(p-value)
% of total genes
D
BMPR1A low
BMPR1A high
E
95% CI
Fitted values
BRCA1 mRNA normalized expression
R²: 0.82
P: <0.0001
BMPR1A protein expression score
F
BMPR1A mRNA (Arbitrary unit)
Wild-type
BRCA1+/-
G
BMPR1B mRNA (Arbitrary unit)
Wild-type
BRCA1+/-

Figure 2

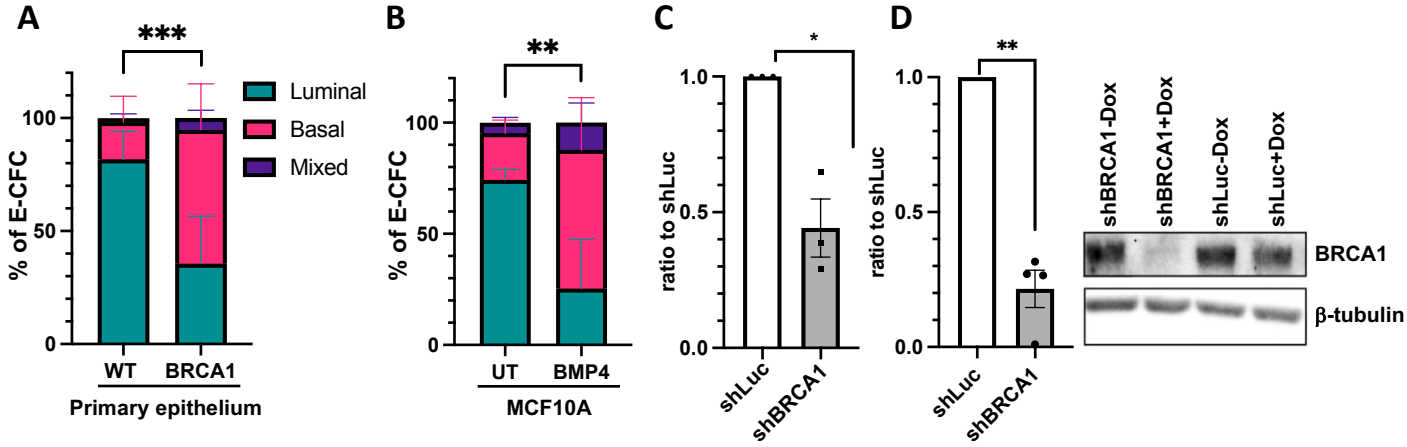
A
***
Luminal
Basal
Mixed
% of E-CFC
100
50
0
WT
BRCA1
Primary epithelium
B
**
% of E-CFC
UT
BMP4
MCF10A
C
*
ratio to shLuc
1.0
0.5
0.0
shLuc
shBRCA1
D
**
ratio to shLuc
shBRCA1-Dox
shBRCA1+Dox
shLuc-Dox
shLuc+Dox
BRCA1
β-tubulin

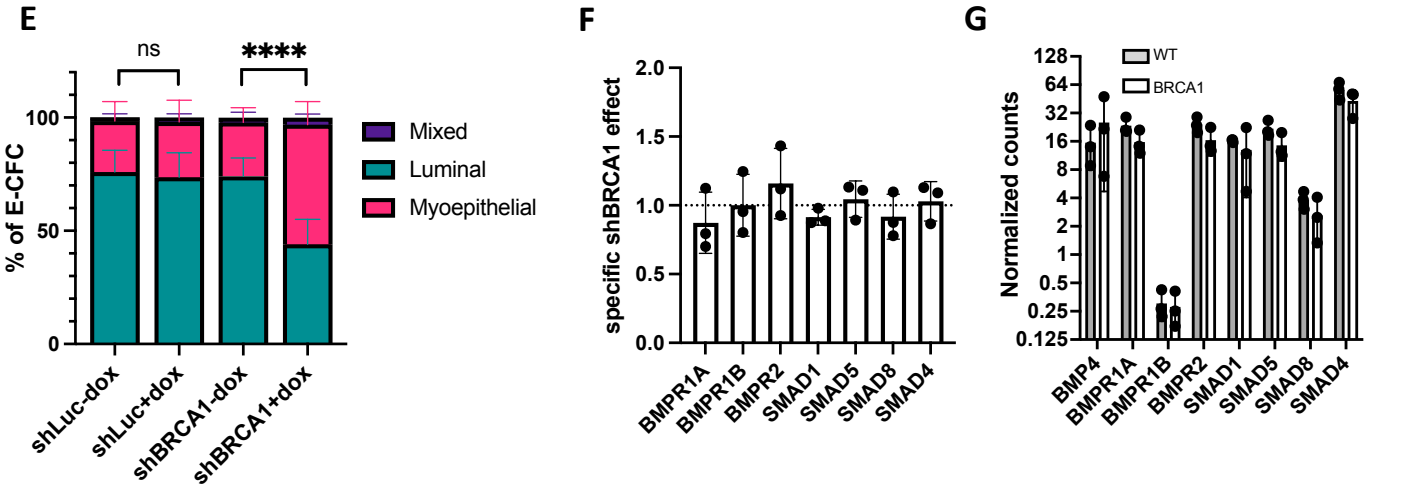
E
ns
****
% of E-CFC
Mixed
Luminal
Myoepithelial
shLuc-dox
shLuc+dox
shBRCA1-dox
shBRCA1+dox
F
specific shBRCA1 effect
2.0
1.5
1.0
0.5
0.0
BMPR1A
BMPR1B
BMPR2
SMAD1
SMAD5
SMAD8
SMAD4
G
WT
BRCA1
Normalized counts
128
64
32
16
8
4
2
1
0.5
0.25
0.125
BMP4
BMPR1A
BMPR1B
BMPR2
SMAD1
SMAD5
SMAD8
SMAD4

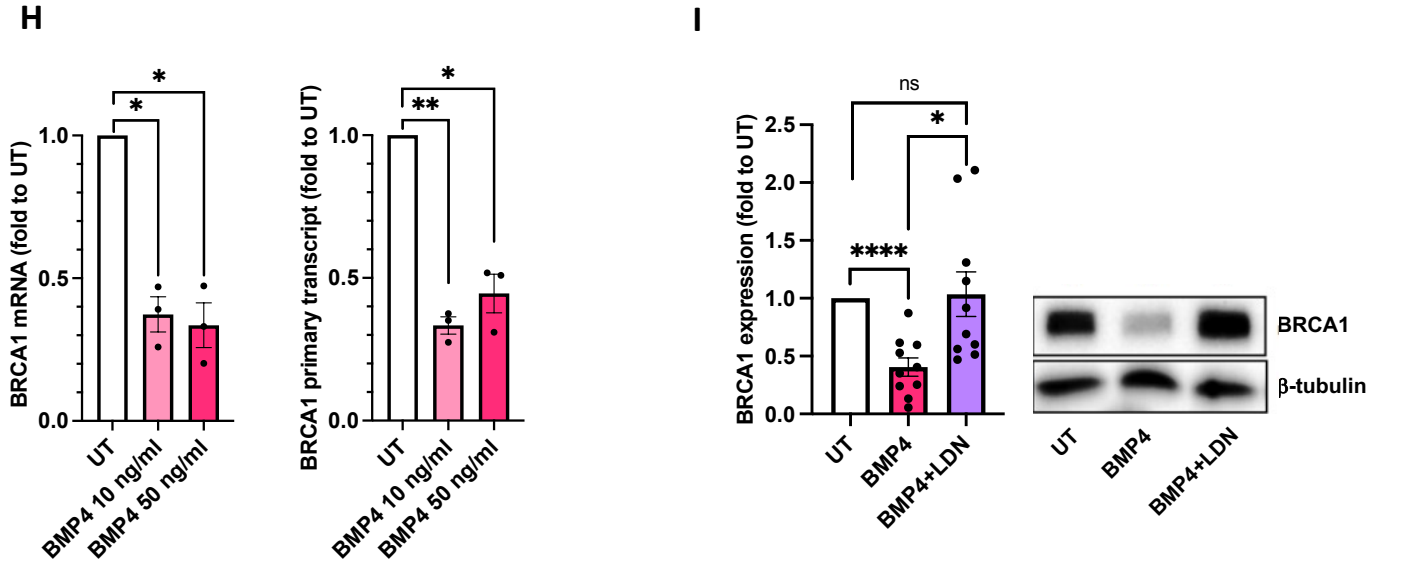
H
*
*
BRCA1 mRNA (fold to UT)
1.0
0.5
0.0
UT
BMP4 10 ng/ml
BMP4 50 ng/ml
*
**
BRCA1 primary transcript (fold to UT)
I
ns
*
****
BRCA1 expression (fold to UT)
2.5
2.0
1.5
1.0
0.5
0.0
UT
BMP4
BMP4+LDN
BRCA1
β-tubulin

Figure 3

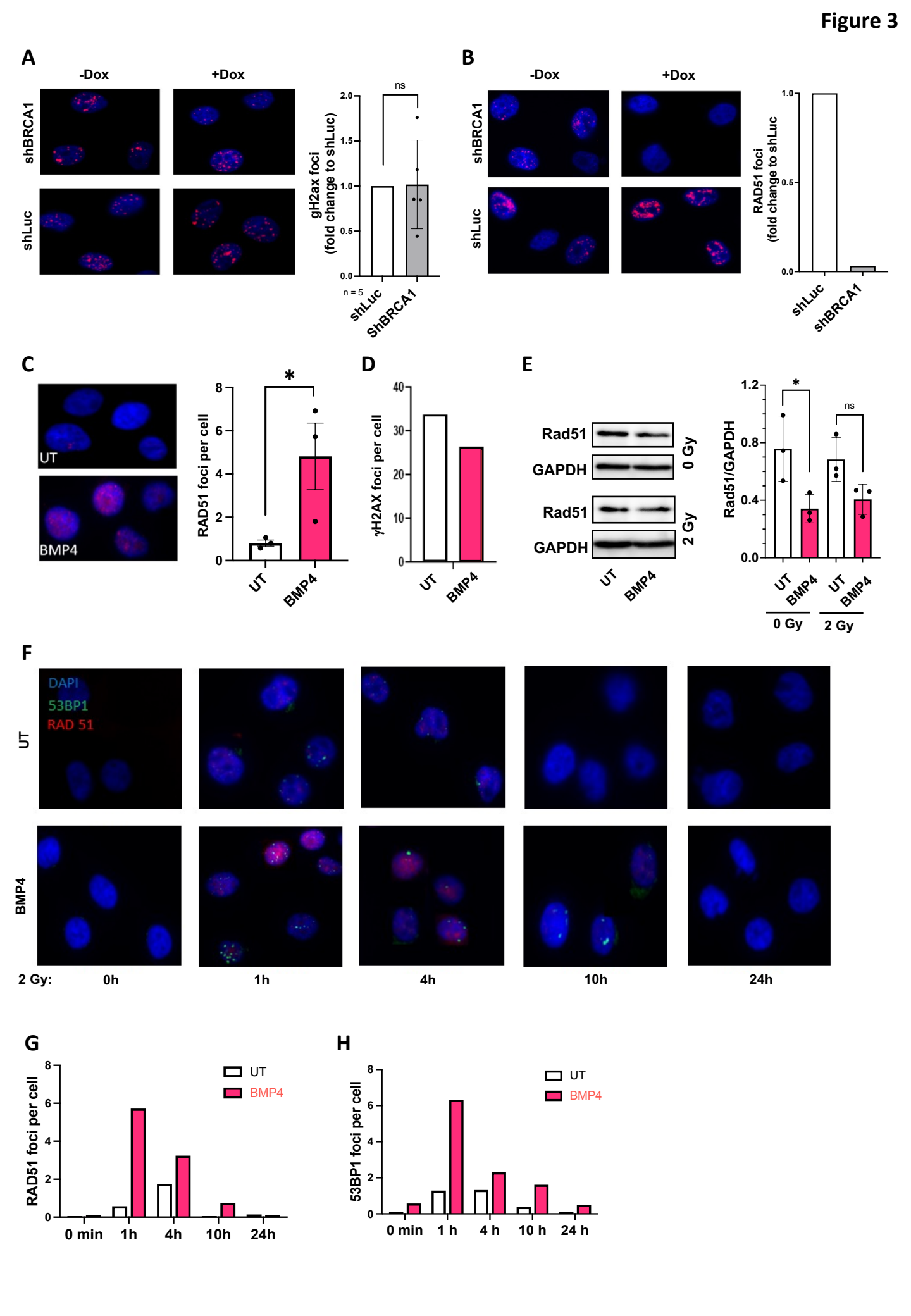
A
-Dox
+Dox
shBRCA1
shLuc
ns
gH2ax foci
(fold change to shLuc)
2.0
1.5
1.0
0.5
0.0
n = 5
shLuc
ShBRCA1
B
-Dox
+Dox
shBRCA1
shLuc
RAD51 foci
(fold change to shLuc
1.0
0.5
0.0
shLuc
shBRCA1
C
UT
BMP4
*
RAD51 foci per cell
8
6
4
2
0
UT
BMP4
D
γH2AX foci per cell
40
30
20
10
0
UT
BMP4
E
Rad51
GAPDH
0 Gy
Rad51
GAPDH
2 Gy
UT
BMP4
Rad51/GAPDH
1.2
0.8
0.4
0.0
*
ns
UT
BMP4
UT
BMP4
0 Gy
2 Gy
F
DAPI
53BP1
RAD 51
UT
BMP4
2 Gy:
0h
1h
4h
10h
24h
G
RAD51 foci per cell
8
6
4
2
0
UT
BMP4
0 min
1h
4h
10h
24h
H
53BP1 foci per cell
8
6
4
2
0
UT
BMP4
0 min
1 h
4 h
10 h
24 h

Figure 4

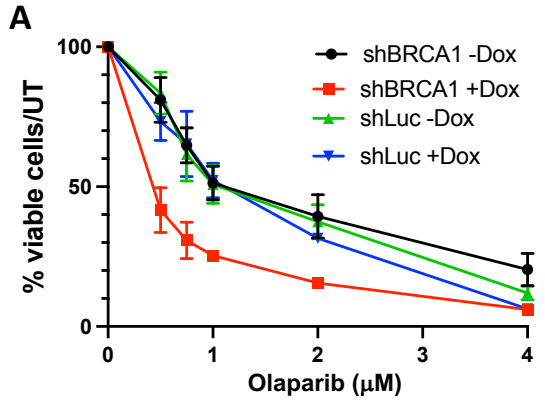

IC 50 estimate, [95% CI] :
shBRCA1 -Dox: 1.20, [0.98 - 1.43]
shBRCA1 +Dox: 0.38, [0.22 - 0.54]
shLuc -Dox : 1.10, [0.92 - 1.28]
shLuc +Dox: 1.02, [0.86 - 1.17]

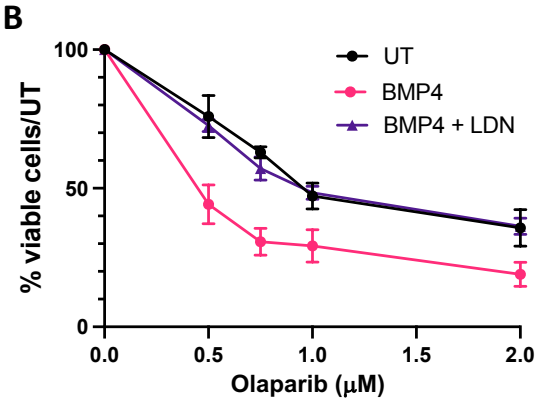

IC 50 estimate, [95% CI] :
MCF10A UT : 1.08, [0.90 - 1.25]
+ BMP4 : 0.37, [0.21 - 0.53]
+ BMP4 + LDN : 1.03, [0.85 - 1.21]

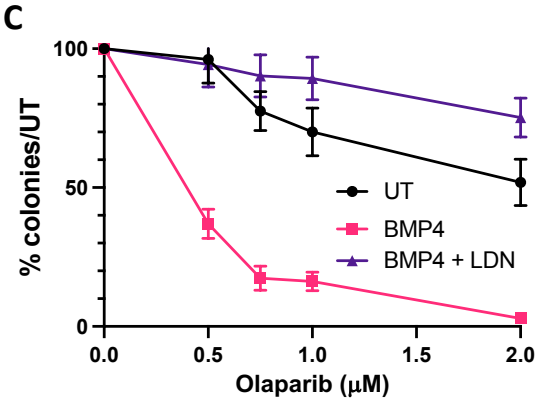

IC 50 estimate, [95% CI] :
MCF10A UT : 2,00, (1.53 – 2.47)
+ BMP4 : 0.32, [0.16 - 0.49]
+ BMP4 + LDN : 4.33, [0.49 – 8,17]

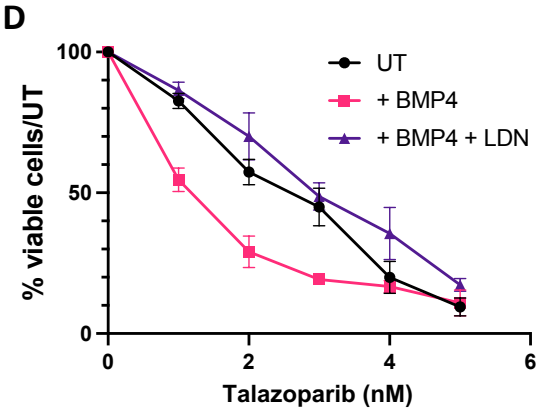

IC 50 estimate, [95% CI] :
MCF10A UT : 2,17 (1.90 – 2.43)
+ BMP4 : 1,11, [0.88 – 1.35]
+ BMP4 + LDN : 2,73, [2,41 – 3,06]

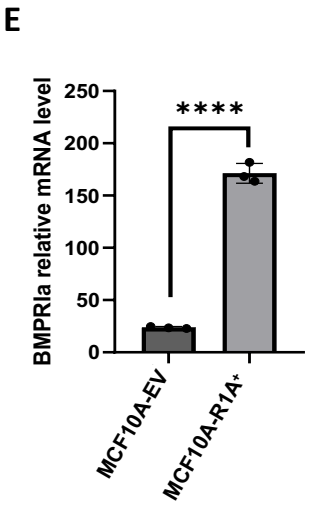

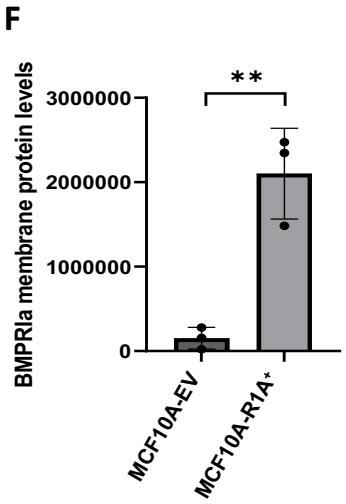

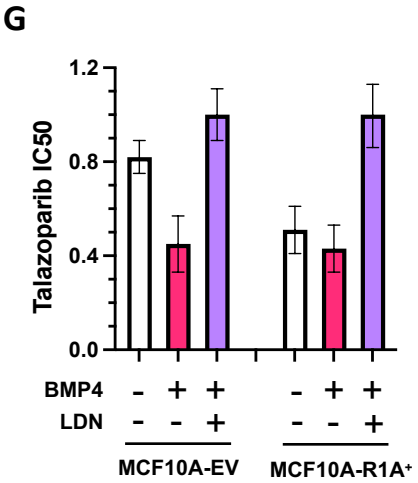

Figure 5

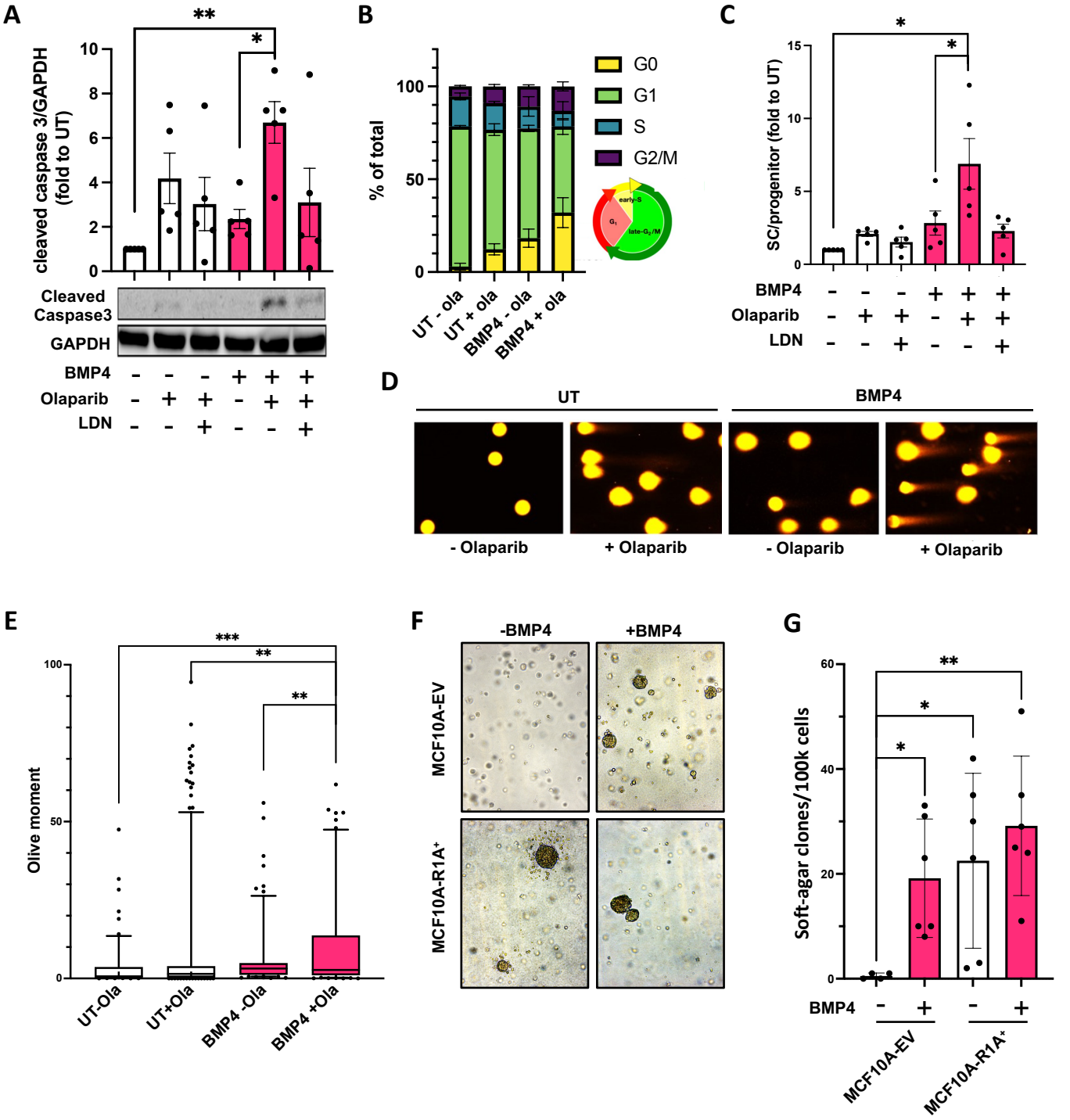
A
cleaved caspase 3/GAPDH (fold to UT)
Cleaved Caspase3
GAPDH
BMP4
Olaparib
LDN
B
% of total
G0
G1
S
G2/M
UT - ola
UT + ola
BMP4 - ola
BMP4 + ola
C
SC/progenitor (fold to UT)
D
UT
BMP4
- Olaparib
+ Olaparib
E
Olive moment
UT-Ola
UT+Ola
BMP4 -Ola
BMP4 +Ola
F
-BMP4
+BMP4
MCF10A-EV
MCF10A-R1A+
G
Soft-agar clones/100k cells
BMP4
MCF10A-EV
MCF10A-R1A+